공학박사 학위논문

Dual-Frequency SSVEP-based BCI for Reducing Eye Fatigue and Improving Classification Rate

낮은 시각 피로도와 높은 정확도를 위한 이중주파수 SSVEP 기반 BCI

2016 년 2 월

서울대학교 대학원

협동과정 바이오엔지니어링 전공

장 민 혜

Dual-Frequency SSVEP-based BCI for Reducing Eye Fatigue and Improving Classification Rate

낮은 시각 피로도와 높은 정확도를 위한 이중주파수 SSVEP 기반 BCI

지도 교수 박 광 석

이 논문을 공학박사 학위논문으로 제출함

2015 년 12 월

서울대학교 대학원

협동과정 바이오엔지니어링 전공

장 민 혜

장민혜의 공학박사 학위논문을 인준함

2016 년 2 월

위 원 장 김 성 완 (인)

부위원장 박 광 석 (인)

위 원 최 진 욱 (인)

위 원 임 창 환 (인)

위 원 박 철 수 (인)

Ph.D. Dissertation

Dual-Frequency SSVEP-based BCI for Reducing Eye Fatigue and Improving Classification Rate

Min Hye Chang

February 2016

Interdisciplinary Program in Bioengineering
The Graduate School
Seoul National University

Dual-Frequency SSVEP-based BCI for Reducing Eye Fatigue and Improving Classification Rate

By

Min Hye Chang

Interdisciplinary Program in Bioengineering
The Graduate School
Seoul National University

This dissertation is approved for
The Degree of Doctor of Philosophy

February 2016

Doctoral Committee:

Chairman _____
Kim, Sungwan, Ph.D.

Vice Chairman _____
Park, Kwang Suk, Ph.D.

Member _____
Choi, Jin Wook, M.D., Ph.D.

Member _____
Im, Chang-Hwan, Ph.D.

Member _____
Park, Cheolsoo, Ph.D.

Abstract

Dual-Frequency SSVEP-based BCI for Reducing Eye Fatigue and Improving Classification Rate

Min Hye Chang
The Interdisciplinary Program in Bioengineering
The Graduate School
Seoul National University

The steady-state visual-evoked potential (SSVEP)-based brain-computer interface (BCI) has been widely investigated because of its high signal-to-noise ratio (SNR), and little requirement for training. However, the stimulus for evoking SSVEP causes high visual fatigue and has a risk of epileptic seizure. Furthermore, stimulation frequency is limited and the SSVEP amplitude diminishes when a monitor is used as a stimulator. In this thesis, a dual-frequency SSVEP is examined to resolve the aforementioned issues. Employing dual-frequency SSVEPs, two novel SSVEP-based BCIs are

introduced to decrease eye fatigue and use harmonic frequencies with increased performance.

First, the spectral characteristics of dual-frequency SSVEPs are investigated and frequency recognition methods for dual-frequency SSVEPs are suggested. Three methods based on power spectral density analysis (PSDA) and two methods based on canonical correlation analysis (CCA) were tested. The proposed CCA with a novel reference signal exhibited the best BCI performance, and the use of harmonic components improved the classification rate of the dual-frequency SSVEP.

Second, the dual-frequency SSVEP response to an amplitude-modulated stimulus (AM-SSVEP) was explored to verify its performance with reduced eye fatigue. An amplitude-modulated stimulus was generated using the product of two sine waves at a carrier frequency (f_c) and a modulating frequency (f_m). The carrier frequency was higher than 40 Hz to reduce eye fatigue, and the modulating frequency ranged around the α-band (9–12 Hz) to utilize low-frequency harmonic information. The feasibility of AM-SSVEP with high BCI performance and low eye fatigue was confirmed through offline and online experiments. Using an optimized combination of the harmonic frequencies, the online experiments demonstrated that the accuracy of the AM-SSVEP was 97%, equivalent to that of the low-frequency SSVEP. Furthermore, subject evaluation indicated that an AM stimulus caused lower eye fatigue and less perception of flickering than a low-frequency stimulus, in a manner similar to a high-frequency stimulus.

Third, a novel dual-frequency SSVEP-based hybrid SSVEP-P300 speller is introduced to overcome the frequency limitations and improve the performance. The hybrid speller consists of nine panels flickering at different frequencies. Each panel contains four different characters that appear in a random sequence. The flickering panel and the periodically updating character evoke the dual-frequency SSVEP, and the oddball stimulus of the target character evokes the P300. Ten subjects participated in offline and online experiments, in which accuracy and information transfer rate (ITR) were compared with those of conventional SSVEP and P300 spellers. The offline analysis revealed that the proposed speller elicited dual-frequency SSVEP. Moreover, the dual-frequency SSVEP significantly improved the SSVEP classification rate and ITR with a monitor in online experiments by 4 % accuracy and 18.8 bpm ITR.

In conclusion, the proposed dual-frequency SSVEP-based BCIs reduce eye fatigue and improve SSVEP classification rate. The results indicate that this study provides a promising approach to make SSVEP-based BCIs more reliable and efficient for practical use.

Keywords : Brain-computer interface (BCI), steady-state visual-evoked potential (SSVEP), dual-frequency, amplitude modulation, hybrid BCI
Student Number : 2009-21075

Table of Contents

List of Tables

List of Figures

List of Abbreviations

AM	Amplitude Modulation
AM-SSVEP	SSVEP response to an amplitude-modulated stimulus
BCI	Brain-Computer Interface
CFC	Customized Frequency Combination
CCA	Canonical Correlation Analysis
DFSSVEP	Dual-Frequency SSVEP
EEG	Electroencephalogram
ERP	Event-Related Potential
ITR	Information Transfer Rate
LDA	Linear Discriminant Analysis
LED	Light-Emitting Diode
PSD	Power Spectral Density
RM-ANOVA	Repeated Measures Analysis of Variance
SN	**S**equence Number
SNR	Signal-to-Noise Ratio
SOA	Stimulus Onset Asynchrony
SSVEP	Steady-State Visual-Evoked Potential
SWLDA	Stepwise Linear Discriminant Analysis

1

Introduction

1.1. Brain-Computer Interface

1.1.1. Basic Concepts

A brain-computer interface (BCI) system decodes a user's intent in order to facilitate communication between the user and the environment using his/her own brain activity. In terms of the measurement methods for brain activity, BCIs can be divided into invasive and noninvasive BCIs [1]. In particular, noninvasive BCIs are primarily based on scalp electroencephalograms (EEGs) because of their low-cost and noninvasive characteristics. Various EEG signals are used for BCI systems, such as sensori-motor rhythm (SMR) [2], event-related potential (ERP) [3, 4], and steady-state evoked potential (SSEP) [5, 6], or combined responses [7]. In particular, steady-state visual-evoked potential (SSVEP) and P300 potential have been widely used for high performance and a relatively large number of commands.

1.1.2. SSVEP-based BCIs

SSVEP is generated in the occipital region when a subject focuses on a target flickering at a constant frequency [8]. SSVEP has peaks at the flickering frequency, its harmonic, and its sub-harmonic frequencies ranging from 1 to 100 Hz [9]. An SSVEP-based BCI utilizes such spectral characteristics. While a user focuses on a flickering stimulus, his/her brain wave is recorded and analyzed using a BCI system. A dominant frequency of the EEG is identified and compared with the flickering frequency. If the dominant frequency is the same or a harmonics of the flickering frequency, the BCI system regards the user as focusing on the corresponding target. If multiple stimuli flicker, the BCI system compare the dominant frequency to the stimulation frequencies, and considers a stimulus with a corresponding stimulation frequency as the one the user focuses on. Because main and harmonic frequencies are all used, the stimulation frequencies should neither overlap nor be harmonics of each other.

SSVEP-based BCI systems have recently attracted growing interest because they require less subject training, offer a higher information transfer rate (ITR), and usually involve a simple system configuration with fewer electrodes than other EEG-based BCI systems [10, 11]. SSVEP-based BCI applications have been proposed for communication with the environment, such as an SSVEP speller [12], control of a hospital bed nursing system [13], or hand orthosis for tetraplegic patients [14].

The stimulation frequency range is divided into low- and medium-frequency bands (< 30 Hz) and high-frequency bands above 30 Hz. SSVEPs in

the low-frequency band have a larger amplitude response than those in the medium- and high-frequency ranges; in particular, SSVEPs at about 15 Hz exhibit the largest amplitude [15]. Therefore, many SSVEP-BCI systems employ the low-frequency band at stimulation frequencies between 8 and 15 Hz [14, 16, 17]. However, low-frequency flickering stimuli are annoying [18] and can cause epileptic seizures. In particular, frequencies within the range of 15–20 Hz pose the greatest risk of seizures. Other frequencies also pose a potential risk of photosensitive epilepsy; however, the percentage of patients with photosensitive epilepsy decreases with increasing flickering frequency [19]. Several recent studies have proposed higher-frequency SSVEP-based BCIs as an alternative to alleviate this risk and visual fatigue [20-22]. However, more people were unable to complete BCI tasks with high-frequency SSVEPs because of their poor performance than those with low-frequency SSVEPs: 84 subjects succeeded in using low-frequency SSVEP-based BCIs, whereas only 56 subjects succeeded with high-frequency SSVEP-based BCIs. Furthermore, high-frequency SSVEPs resulted in significantly lower accuracy and ITR [22]. Even within a high-frequency band, the detection accuracy decreased by 8.6% as the stimulation frequency increased from 30 Hz to 45 Hz [21].

Various stimuli are used for SSVEP-based BCIs, such as light-emitting diodes (LEDs), and liquid crystal display (LCD) and cathode ray tube (CRT) monitors [23]. An LED stimulator can generate a great number of stimuli with small frequency steps and various waveforms of the signal (e.g., sine, rectangular, or modulated waveform). The peak power of an SSVEP evoked by

LEDs is higher than that evoked by LCD and CRT monitors [23]. However, the stimulator and signal processor are separate and complex, whereas, a monitor can provide both stimulation and feedback without an additional device. A stimulus that flickers as black and white is generated on the basis of the monitor's refresh rate; thus, the stimulation frequency is limited to

$$Stimulation\ frequency\ of\ a\ monitor = Refresh\ rate\ /\ N, \quad (1)$$

where N indicates an integer larger than 2. A recent study developed a dynamically optimized SSVEP speller producing 36 stimuli with only six flickering frequencies in frequency-limited condition [24]. Another study reported a 45-target monitor-based SSVEP-BCI system in which the brightness of a stimulus varied sinusoidally [25], thus it did not follow (1). However, in those systems, harmonic frequencies still could not be used for different stimuli. Furthermore, the SSVEP peak is weaker than that evoked by LEDs. These limitations reduce the ITR.

1.1.3. P300-based BCIs

The P300 potential is elicited approximately 300 ms after a subject spots an infrequent target. When a subject detects a stimulus change, the neural stimulus representation updates in working memory and the P300 component is produced in the ERPs [26]. P300 has two subcomponents: P3a and P3b. P3b is the "classic" P300 which is elicited by deviant items when a subject is concentrating on the stimuli. P3b peaks at approximately 300 ms and is a maximum at the parietal region. P3a is elicited by novel stimuli that is exceedingly rare and has no previously formed memory template (novel stimuli). P3a is a maximum at the frontal or central region [27]. Both components can be used for P300-based BCIs [28].

The oddball paradigm is commonly used for P300-based BCIs, which presents an infrequent target in the background of frequent standard stimuli. Various P300-based BCI systems have been designed, including a visual character speller [3], an auditory speller [29], and an auditory BCI with natural stimuli [30]. Some of the systems have already been tested with neuromuscular patients [31].

Usually, P300-based BCIs could have many targets, which can increase system speed in proportion to the number of targets. However, P300-based BCIs need repetitive stimulation sequences to average ERPs, which increases the stimulation time and reduces ITR [3]. Furthermore, because of high intra-subject variability, a training session is required to operate the system.

1.1.4. Hybrid SSVEP-P300 BCIs

Complementary strategies that combine P300 and SSVEP offer a more reliable and faster BCI speller. A hybrid BCI system designed for practical use in asynchronous control has been described [32]. The system employed P300 and SSVEP as a brain switch to control a real wheelchair; nonetheless, the speed of the BCI was not improved. A visual parallel-BCI speller incorporating P300 and SSVEP-blocking (SSVEP-B) features has been suggested as a way to improve the speller's accuracy and ITR [33, 34]. However, this system requires that the SSVEP stimulation be suspended for a certain period to generate the P300 potential, and this time gap can attenuate the SSVEP. Furthermore, harmonic frequencies cannot be used for creating more targets. The limited number of flickering frequencies may increase the number of flashes in a sequence and the stimulation time for P300 and decrease ITR. A hybrid BCI spelling system has been developed that divides a conventional P300 speller into six subgroups, where each group flickers at different frequencies [35]. The hybrid system combines the individual features of P300 and SSVEP to reduce errors occurring in the same row or column relative to the target. The same research team has proposed another hybrid SSVEP-P300 BCI speller to decrease the flash number for P300 by half, which increases the accuracy and ITR compared to the SSVEP and P300 spellers [36]. However, these systems do not solve the frequency-limitation problem of the SSVEP-based BCI system.

1.2. Motivation and Objectives

SSVEP-based BCIs have advantages over other EEG-based BCIs: 1) they need almost no subject training; thus, they are easy to implement. 2) They have low inter- and intra-subject variability; simple signal processing techniques can lead to high performance. 3) Accuracy is relatively high with short EEG signals, resulting in high ITR.

However, flickering visual stimuli cause eye fatigue and have a high potential for epileptic seizure in the low-frequency range. Efforts to reduce visual fatigue created a half-field stimulation pattern without direct attention to a stimulus [37] or a high duty-cycle flicker with an α-band flashing frequency [38]. However, these stimuli also flicker at a low frequency; thus, visual discomfort (annoyance and fatigue) and the risk of seizure caused by a low-frequency flicker cannot be completely eliminated.

Another problem is that the stimulation frequency with a monitor is limited, and even harmonic frequencies cannot be used in the frequency-limited condition. The low number of available stimulation frequencies reduces the number of targets, and consequently results in low ITR.

The dual-frequency SSVEP-based BCI can be an alternative to single-frequency SSVEPs to complement the aforementioned weaknesses. Spectra peaks of a dual-frequency SSVEP appear at a linear combination of stimulation frequencies. Thus, a dual-frequency stimulus with a high frequency can theoretically evoke a low-frequency SSVEP. Then, the high stimulation frequency can reduce eye fatigue without damage to SSVEP amplitude by

generating a low-frequency harmonic component. On the other hand, if one of the stimulation frequency pair changes, the spectral peaks of the corresponding dual-frequency SSVEP change. Thus, the same or harmonic frequency can be used for different stimuli with a different frequency pair.

However, characteristics of dual-frequency SSVEPs, such as harmonic components varying with stimulation frequencies or inter- and intra-subject variability, have rarely been reported. Furthermore, dual-frequency SSVEP-based BCIs using its harmonics as well as fundamental frequencies have not been investigated. Therefore, a feasibility study on dual-frequency SSVEP-based BCIs should be performed to investigate the issues and to develop a signal processing method for a dual-frequency SSVEP-based BCI system.

In this thesis, a standard dual-frequency SSVEP-based BCI system is investigated to identify the spectral characteristics of dual-frequency SSVEPs and establish a frequency recognition method that considers harmonic components as well as main frequencies. Then, two novel dual-frequency SSVEP-based BCI systems are proposed, each of which was designed to solve the aforementioned issues as follows:

- Amplitude-modulated stimulation with different combinations of carrier and modulation frequencies was designed to reduce eye fatigue without degradation of performance. The visual stimulus was generated according to the double-sideband suppressed carrier (DSB) signal, which flickered at a high frequency while

also carrying low-frequency information. The effect of the two frequency bands can be identified by the amplitude of the SSVEP and the level of eye fatigue.

- A novel hybrid BCI speller that generates dual-frequency SSVEPs was developed to present characters periodically while simultaneously flickering. The hybrid stimulus consists of a stimulation-frequency pair for SSVEP and P300. Thus, harmonic flickering frequencies can be used for different stimuli with relatively prime stimulation frequencies for P300. Furthermore, the simultaneous stimulation by the proposed speller can reduce the time required for stimulation, which results in a swift decision.

2

Frequency Recognition Methods for DFSSVEP-based BCI

2.1. Basic Concepts

A dual-frequency SSVEP-based BCI system has been suggested for generating more stimuli with a few flickering frequencies, contrary to a single-frequency SSVEP-based BCI system where the number of targets should be the same as the number of flickering frequencies [39]. Through a combination of the frequencies, N flickering frequencies can theoretically generate ${}_{N}C_{2} + N$ stimuli. Thus, employing dual-frequency SSVEPs can benefit in frequency-limited settings such as the utilization of a monitor [40]. Most dual-frequency stimulators generate light intensity variation as a sinusoidal or square wave. However, neither periodic shape variation nor a combination of shape and intensity variations has been used.

A dual-frequency SSVEP has spectral peaks in a linear combination of the two stimulation frequencies as well as main frequencies. Moreover, the appearance of the harmonics varies with stimulation condition. In [39], in response to a dual-frequency stimulus flickering at different frequencies (f_1 and f_2), spectral peaks occurred at the symmetric harmonic frequencies: $2f_1 - f_2$ and $2f_2 - f_1$. In [40], flickering frequencies for the dual-frequency stimulus were in the low-frequency band, less than 5 Hz, and the SSVEP peak appeared at the sum of the frequencies. With a different frequency set and various stimulus shapes (Figure 2-1), harmonic frequencies were found at $|f_1 - f_2|$, $3f_1 - f_2$, and $3f_2 - f_1$ [41]. In the case of a dual-frequency stimulation consisting of two harmonic frequencies, a corresponding SSVEP concentrates the power at one of the frequencies [42]. The study about dual-frequency SSVEP-based BCI was published as a conference paper [43].

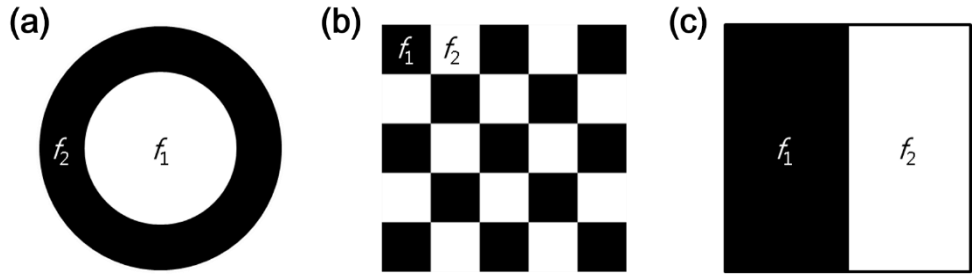

Figure 2-1. Three different shapes of stimuli for evoking a dual-frequency SSVEP, (a) concentric circle, (b) checkerboard, and (c) square [41]

Bieger and Molina [44] suggested multi-frequency stimulation generated by the sum or average of multiple pure frequency stimulations. These authors assumed that such stimulation would elicit SSVEPs at linear combinations of the stimulus frequencies, but did not demonstrate their theory. Teng et al. [45] investigated EEG responses to multi-frequency sine stimulation at two or three frequencies. However, they examined only which stimulus frequency was dominant in an SSVEP according to different frequency combinations without a BCI application. The analysis of the resulting SSVEP peaks was limited to the main stimulus frequencies and not the harmonic frequencies, unlike the present study. In addition, the stimulus frequencies tested were below 20 Hz, which is sufficient to cause considerable eye fatigue. Lopez et al. [46] used AM stimuli similar to those used in this study; however, all of the stimuli had the same carrier and modulation frequencies of 16 Hz and 1 Hz, respectively; the only difference was the phase shift. The acquired EEG signals were AM demodulated before an SSVEP recognition step. Therefore, the visual response evoked by AM visual stimulation was not considered in the SSVEP analysis, and advantages obtained from using the multi-frequency stimulation could not be expected in their approach. Shyu et al. [39] reported that a dual-frequency SSVEP can be evoked through a stimulus consisting of two LEDs flickering at different frequencies. The approach has the advantage of generating more stimuli with the limited number of available flickering frequencies using the combination of the frequencies. When a subject was exposed to the stimulus flickering at both f_1 and f_2, the symmetric harmonic frequencies (i.e., peak

frequencies of dual-frequency SSVEP) were f_1, f_2, $2f_1 - f_2$, and $2f_2 - f_1$. However, their findings were not applied to BCI systems.

2.2. DFSSVEP Recognition Methods

SSVEP is a periodic evoked potential elicited by a visual stimulus flickering at a constant frequency, showing peaks at multiple harmonic frequencies such as the main, second, or sub-harmonic frequency [9]. SSVEP-based BCIs classify SSVEP segments by exploiting such spectral characteristics. The most used frequency recognition methods for SSVEP are power spectral density analysis (PSDA) and canonical correlation analysis (CCA). In the previous study, CCA and PSDA were compared for online multi-channel SSVEP-based BCI, and CCA was superior to PSDA [5].

Even though some research groups have reported characteristics of dual-frequency SSVEPs, a dual-frequency SSVEP-based BCI system has rarely been implemented. To our knowledge, a classification strategy for dual-frequency SSVEP has not been investigated using both main and harmonic frequencies. Conventional frequency recognition methods are optimized for single-frequency SSVEP. Contrary to single-frequency SSVEP, dual-frequency SSVEP can have multiple peaks at linear combinations of stimulation frequencies, and a distinct peak frequency or amplitude even varies between individuals [47]. Therefore, the existing classification methods for single-frequency SSVEPs should be equipped to handle the variation.

In this section, modified PSDA and CCA were examined for dual-frequency SSVEP classification. The three new methods used conventional features (SNR or correlation) and classification methods (ranking or linear discriminant analysis, LDA). The other two methods used modified features

contributed by both main and harmonic frequencies, taking advantage of harmonic frequencies.

2.2.1. PSDA-based Methods

PSDA usually calculates spectral power or signal-to-noise ratio (SNR) of SSVEP at harmonic frequencies. The *n*-th order SSVEP-SNR is calculated as

$$\mathrm{SNR}(f) = \frac{n \times P(f)}{\sum_{k=1}^{n/2} [\mathrm{P}(f + k\Delta f) + \mathrm{P}(f - k\Delta f)]}, \quad (2)$$

where f denotes frequency, P represents the power of the signal, and Δf indicates the frequency step. SSVEP classification is accomplished by choosing the largest value among those of stimuli [48] or using a classifier such as linear discriminant analysis (LDA) [49].

Three different frequency recognition methods were devised for PSDA (Table 2-1): 1) *SNR-ranking*, 2) *SNR-sum*, and 3) *SNR-LDA*.

The first method is to select two frequencies with the largest SNRs among the main frequencies. SSVEP-SNR is calculated at each stimulation frequency; then the stimulation frequencies are arranged in descending order of SNR. Because dual-frequency stimuli are composed of a combination of two frequencies, the first two frequencies in the rank are further compared with the stimulation-frequency-pairs. If the frequency set selected does not correspond to any of the stimulation frequency pairs, the classification is considered failed.

The second method is to compare the sum of SNRs at the two main frequencies and the harmonic frequencies. The SNR values are summed for each class at the main frequencies ($SNR_{i,f1}$, $SNR_{i,f2}$) and with or without the combination of the harmonic frequencies ($SNR_{i,f\text{harm}}$):

$$SNRsum_i = SNR_{i,f1} + SNR_{i,f2} + SNR_{i,f\text{harm}}, \qquad i = 1, 2, 3, 4 \tag{3}$$

where i indicates the class. The class with the largest SNR sum is determined as the target on which the subject focuses. When including harmonic frequencies, classification accuracies of all combinations are compared, and the maximum accuracy with a specific combination becomes the representative classification rate of a specific time.

The last modified PSDA method is to apply LDA with features of SNR values at the main frequencies and the combination of the harmonic frequencies. LDA estimates hyperplanes to separate the data of multiple classes. This technique has a low computational requirement, suitable for an online BCI system [50]. As in the *SNR-sum* method, only the maximum accuracy with a specific combination of harmonic frequencies is considered for performance comparison.

Table 2-1. Modified frequency recognition methods for dual-frequency SSVEPs

Method	Feature	Classification
SNR-ranking	SNR at each stimulation frequency	Select two stimulation frequencies with the largest SNR
SNR-sum	Sum of SNRs at stimulation and non-integer harmonic frequencies	Select a frequency set with the largest SNR sum
SNR-LDA	SNRs at stimulation and non-integer harmonic frequencies	Select a frequency set with the largest classifier score
Correlation-ranking	Correlations between EEG and conventional reference signal for each stimulation frequency	Select two stimulation frequencies with the largest correlation
CCA with a novel reference signal	Correlations between EEG and novel reference signal for each stimulus	Select a frequency set with the largest correlation

2.2.2. CCA-based Methods

CCA is a widely used approach to recognize SSVEPs [5, 51]. This approach finds a pair of linear transformations (W_X and W_Y) for multichannel EEG (X) and reference signal (Y) by maximizing the correlation (ρ) between the two projections (i.e., the canonical variants $x = X^T W_X$ and $y = Y^T W_Y$) of the canonical variables (X and Y) [5]:

$$\max_{W_x, W_y} \rho(x, y) = \frac{E[x^T y]}{\sqrt{E[x^T x]E[y^T y]}} = \frac{E[W_x^T X Y^T W_y]}{\sqrt{E[W_x^T X X^T W_x]E[W_y^T Y Y^T W_y]}}. \quad (4)$$

Because multidimensional sets can be used as the variables, multichannel EEG data can be simply analyzed using CCA [5].

When applying CCA to a BCI system, X refers to t_ws-long N_{ch}-channel EEG signals, and Y refers to the set of reference signals with the same length as X. The conventional reference signal Y_f consists of both the *sine* and *cosine* of N_h harmonics of frequency f:

$$Y_f = \begin{pmatrix} \sin(2\pi f t) \\ \cos(2\pi f t) \\ \sin(4\pi f t) \\ \cos(4\pi f t) \\ \vdots \\ \sin(2\pi N_h f t) \\ \cos(2\pi N_h f t) \end{pmatrix} \quad (5)$$

The stimulus where the user focused is classified as

$$\mathrm{C} = \max_{i} \rho_i , \qquad i = 1, 2, \ldots, K, \tag{6}$$

where K is the number of targets. For example, if four visual stimuli constitute a BCI system, four Y_f values corresponding to each stimulus are estimated. The linear combinations that maximize canonical correlations between an SSVEP segment and each Y_f are estimated. The four canonical correlations of the individual Y_f are compared, and the class with the maximum correlation is assumed to be the watched target.

Two modified CCAs are designed for dual-frequency SSVEP classification (Table 2-1): 1) *correlation-ranking*, and 2) *CCA with a novel reference signal*. Because a conventional reference signal consists of a *sine* and *cosine* at a specific frequency, direct multi-frequency recognition is not possible with *correlation-ranking*. Therefore, the method calculates the correlation for each stimulation frequency and compares the values. As with the *SNR-ranking* method, a stimulus with stimulation frequencies with the largest correlations is regarded as a target the user focuses on.

The second modified CCA uses a novel reference signal for directly recognizing multi-frequency components of dual-frequency SSVEP. Compared with *correlation-ranking*, a novel reference signal consists of *sine* and *cosine* at multiple frequencies including two main frequencies (f_1 and f_2), non-integer harmonic frequencies ($f_{NI\text{-}Harm}$), and their second harmonics:

$$Y_{dual} = \begin{pmatrix} \sin(2\pi f_1 t) \\ \cos(2\pi f_1 t) \\ \sin(4\pi f_1 t) \\ \cos(4\pi f_1 t) \\ \sin(2\pi f_2 t) \\ \cos(2\pi f_2 t) \\ \sin(4\pi f_2 t) \\ \cos(4\pi f_2 t) \\ \sin(2\pi f_{NI-Harm} t) \\ \cos(2\pi f_{NI-Harm} t) \\ \sin(4\pi f_{NI-Harm} t) \\ \cos(4\pi f_{NI-Harm} t) \\ \vdots \end{pmatrix} \quad (7)$$

A reference signal is estimated for each class, and a correlation is calculated for a class. The class with the largest correlation is finally chosen, as with the conventional CCA.

2.3. Offline Analysis

2.3.1. Dual-Frequency Stimulus

A dual-frequency stimulus consisted of two LED arrays that flickered as sine waves at different frequencies (f_1 and f_2; Figure 2-2). A diffusion film was attached above the arrays so that subjects could focus on the stimulus without focusing on either of them. The flickering frequencies were non-harmonic and in the medium- or high-frequency range: 19 Hz, 23 Hz, 27 Hz, and 31 Hz. Four pairs of them were used for generating dual-frequency stimuli: (19 Hz, 27 Hz), (19 Hz, 31 Hz), (23 Hz, 27 Hz), and (23 Hz, 31 Hz).

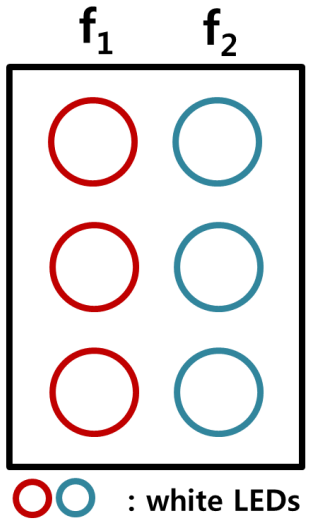

Figure 2-2. A dual-frequency stimulus composed of two LED arrays flickering at f_1 and f_2, respectively

2.3.2. Experimental Settings

Three subjects (two males and one female) participated in the experiment with informed consent. They had corrected-to-normal vision and no experience or family history of epileptic seizure.

At the beginning of a trial (t = 0 s), a subject was requested to gaze at a cross in the center of a 26-inch monitor (T260HD, Samsung, Korea). When an arrow that headed for a target was presented (t = 3 s), a subject had to focus on the relevant stimulus for 6 s. While focusing on the target, eye or jaw movement was not allowed, to avoid noise. Every target was focused on ten times equally in random sequence. For EEG analysis, the first 0.5 s signal of the 6 s EEG was rejected to exclude noise generated from eye or neck movement to locate a target.

A two-channel EEG signal was achieved using g.USBamp (g.tec, Austria) at O1 and O2, well known for engaging in SSVEP generation [8]. The reference and ground electrodes were positioned at A1 and Fpz, respectively. The sampling rate was 512 Hz, and a high-pass filter at 2 Hz and a notch filter at 60 Hz were applied on the amplifier.

2.3.3. Spectral Analysis of DFSSVEP

A spectrum was estimated for each target and each subject using g.BSanalyze (g.tec, Austria) to identify harmonic frequencies of the dual-frequency SSVEP. The "spectrum" function first detrended and windowed a 5-s-length EEG signal, and estimated the square of the value of the fast Fourier transform (FFT). The power spectral density (PSD) of each target was used to estimate the signal-to-noise ratio (SNR) of the SSVEP as in (2). A frequency with SNR larger than 3 was identified as a peak frequency. Then, the peak frequencies of each target were compared to define the harmonic components of the dual-frequency SSVEP. A frequency component found in the spectra of the targets in common was defined as a harmonic component of the dual-frequency SSVEP. Every possible combination of the harmonic components was employed as a feature, as in 2.2. Considering the effect of main frequencies, the combination always included two main frequencies.

2.3.4. Signal Processing

The length of an EEG segment was varied from 1 s to 5 s. The segment was extracted using a rectangular window starting at every second of each trial. For example, a 1-s segment was extracted from each trial starting at 3.5 s, 4.5 s, 5.5 s, 6.5 s, and 7.5 s.

In the classification process, ten-fold cross-validation was used. BCI performance was estimated as the average accuracy of the ten validation sets. Classification accuracies were statistically compared using analysis of variance (ANOVA) with $\alpha = 0.05$. For the *SNR-sum*, *SNR-LDA*, and *CCA with a novel reference signal* methods, classification results with or without non-integer harmonics were statistically compared.

2.4. Results

2.4.1. Harmonic Frequency

Peak frequency components were different for targets and subjects. For example, a spectrum of target 1 of subject 1 peaked at 19 Hz (f_1), 27 Hz (f_2), 35 Hz ($2f_2 - f_1$), 38 Hz ($2f_1$), and 46 Hz ($f_1 + f_2$), whereas a spectrum of target 2 of subject 1 peaked at 19 Hz (f_1), 31 Hz (f_2), 12 Hz ($f_2 - f_1$), 57 Hz ($3f_1$), and 62 Hz ($2f_2$), and a spectrum of target 2 of subject 3 peaked at 19 Hz (f_1), 23 Hz, and 46 Hz. Peak frequency components found in common and related to the main frequencies were defined as harmonic components of dual-frequency SSVEP. The peaks appeared at 23 Hz and 46 Hz in the spectrum of target 2 of subject 3 were not related to the main frequencies (19 Hz and 31 Hz); thus, they were not considered as harmonic components. Finally, four harmonic components were identified as $2f_1 - f_2$, $2f_2 - f_1$, $f_1 + f_2$, and $|f_1 - f_2|$. Sixteen combinations of the four harmonic components were tested for the *SNR-sum*, *SNR-LDA*, and *CCA with a novel reference signal* methods.

2.4.2. Comparison of Recognition Rates

Table 2-2 shows average accuracy according to the classification condition. Classification methods based on CCA significantly outperformed those on PSDA by 11.6 ± 3.4% (*t*-test, $t = 4.332$, $p < 0.001$). *SNR-ranking* was significantly inferior to the others ($p < 0.001$), and *CCA with a novel reference signal* showed significantly higher accuracy than the others except *SNR-LDA* ($p < 0.02$). Classification considering harmonic components resulted in better performance than that with only main frequencies (*t*-test, $t = 3.124$, $p = 0.002$). Accuracy increased as window length increased ($F = 106.636$, $p < 0.001$), and there was an interaction between window length and classification method ($F = 2.604$, $p = 0.023$).

Accuracies of the *SNR-sum*, *SNR-LDA*, and *CCA with a novel reference signal* methods were compared with factors of window length and frequency combination using repeated-measures ANOVA (RM-ANOVA; Figure 2-3). All methods showed a significant difference in accuracies according to window length ($F = 17.430$, $p = 0.026$ for *SNR-sum*; $F = 72.066$, $p = 0.001$ for *SNR-LDA*; $F = 35.530$, $p = 0.017$ for *CCA with a novel reference signal*). However, a significant difference between accuracy with or without harmonics existed for *SNR-sum* and *SNR-LDA* ($F = 23.672$, $p = 0.04$ for *SNR-sum*; $F = 446.459$, $p = 0.002$ for *SNR-LDA*). No interaction was observed.

Table 2-2. Average Accuracies in terms of features, classification methods, frequency combinations, and window lengths

Category	Subcategory	Average accuracy (%)
Feature	SNR (PSDA)	57.7 ± 13.4
	Correlation (CCA)	69.4 ± 16.8
Classification method	SNR-ranking	31.5 ± 17.6
	SNR-sum	62.5 ± 13.0
	SNR-LDA	66.1 ± 11.9
	Correlation-ranking	60.0 ± 18.5
	CCA with a novel reference signal	74.1 ± 14.0
Frequency combination	Without harmonics	63.3 ± 13.4
	With harmonics	71.9 ± 12.8
Window length	1 s	43.7 ± 12.5
	2 s	58.3 ± 15.4
	3 s	63.9 ± 17.5
	4 s	70.6 ± 17.1
	5 s	74.1 ± 16.4

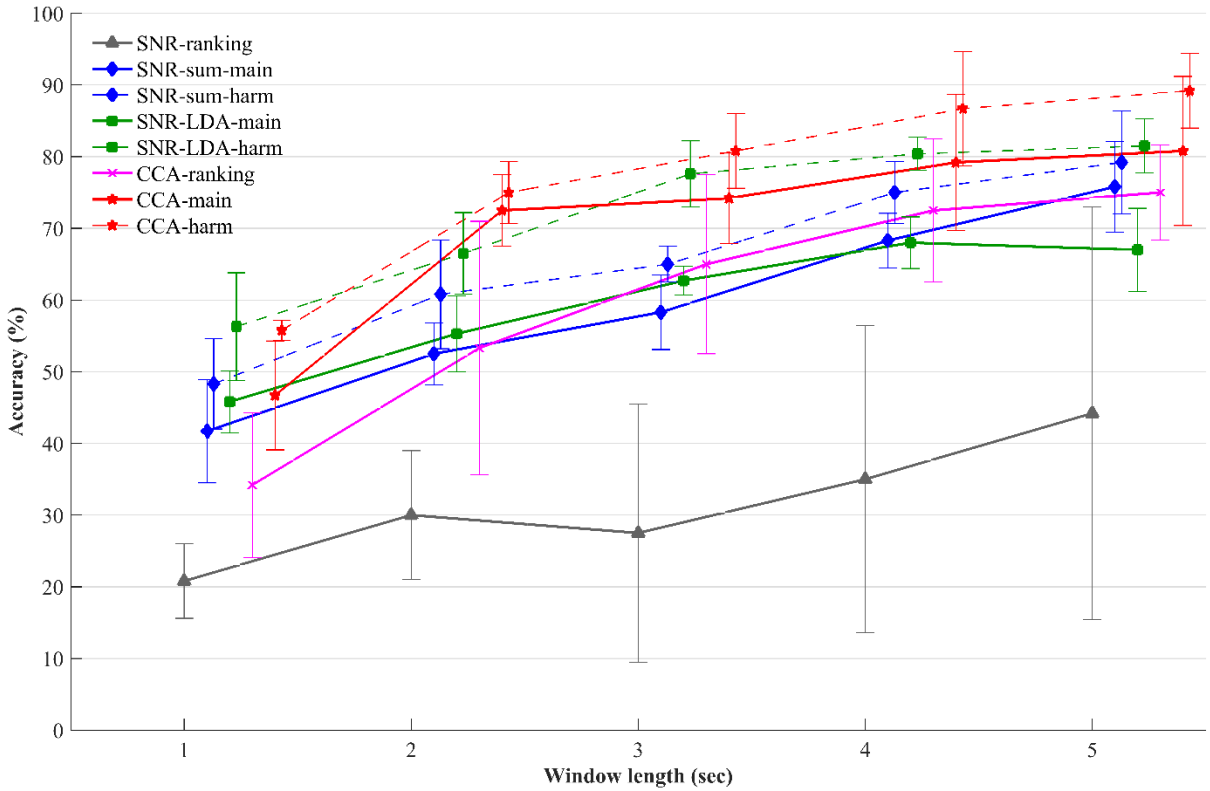

Figure 2-3. Classification rate according to classification methods and window lengths

2.5. Conclusion

In this section, a dual-frequency SSVEP-based BCI was examined with five classification methods. Stimulation frequencies overlapped for stimuli; thus, conventional classification techniques for single-frequency recognition should be modified for multiple-frequency recognition. The best classification method (*CCA with a novel reference signal*) classified dual-frequency SSVEPs with an accuracy of approximately 90%, which was higher than the others. These results implied that *CCA with a novel reference*—especially with harmonic components—would be better than PSDA for dual-frequency SSVEP as conventional CCA was for single-frequency SSVEP [5]

The proposed method (*CCA with a novel reference signal*) was devised to classify multi-frequency SSVEPs at once. In the other methods, even though SNR or correlation is estimated at each stimulation frequency, an additional classification step, such as LDA, is required because a dual-frequency stimulus consists of multiple frequencies. If harmonic components are considered, features will be required as many as the number of harmonic frequencies. However, no matter how many frequencies are employed, only N features are required to classify N classes for *CCA with a novel reference signal*. Furthermore, all of the harmonic frequencies contributed to the frequency recognition; thus, the method is robust to intra-subject variability as in 2.4.1..

3

DFSSVEP-based BCI for Reducing Eye Fatigue

3.1. Basic Concepts

3.1.1. Amplitude Modulation Technique

Amplitude modulation (AM) techniques have been widely used in electronic communication, mostly for radio carrier waves. An amplitude-modulated signal is presented as the amplitude variation of a carrier signal in accordance with the amplitude and frequency variations of the modulating signal. In particular, DSB signals suppress the carrier to reduce the consumption of power. While a general amplitude modulation signal simultaneously contains spectral peaks at the carrier frequency and in the upper and lower sidebands, a DSB signal contains peaks only at the frequencies in the sidebands [52]. If the brightness of a visual stimulus varies as a DSB-AM sine wave, the maximum and minimum brightness of a stimulus flickering at the carrier frequency will change sinusoidally at the modulating frequency. With the carrier frequency in

the high-frequency band and the modulating frequency in the low-frequency band, a DSB-AM stimulus can convey high- and low-frequency information simultaneously. If a brain responds to both types of information, the AM-SSVEP would contain peaks in a wide frequency range from low to high frequencies. Then, the AM stimulus would encompass the advantages of both low-frequency SSVEPs, such as high amplitude and low BCI illiteracy, and high-frequency SSVEPs, such as less eye fatigue and a decreased risk of epileptic seizure.

Several research groups have introduced various types of combined frequency stimulation methods analogous to AM stimulus as in 2.1. However, harmonic components elicited by multi-frequency stimuli were not analyzed and utilized for BCI systems. Moreover, the eye fatigue problem caused by low-frequency flickering stimuli was not considered.

3.1.2. Amplitude-Modulated Stimuli for Evoking AM-SSVEP

At time t, a simple carrier (c(t)) is given as a sine wave at carrier frequency (f_c):

$$c(t) = \sin(2\pi f_c t). \quad (8)$$

Here, a modulating signal (m(t)) is a sine wave with modulation frequency (f_m):

$$m(t) = \sin(2\pi f_m t). \quad (9)$$

Then, the AM stimulus, S(t), is simply expressed as the product of c(t) and m(t) to generate a DSB signal. Using trigonometric functions yields

$$S(t) = c(t)m(t) = -\frac{1}{2}[\cos(2\pi(f_c + f_m)t) - \cos(2\pi(f_c - f_m)t)]. \quad (10)$$

From this equation, the spectrum of S(t) has peaks at $f_c + f_m$ and $f_c - f_m$. In this study, the f_cs were high frequencies exceeding 40 Hz to reduce eye fatigue and f_ms were low frequencies near the α-band (9–12 Hz) to achieve a large SSVEP amplitude such that high-frequency stimuli carrying low-frequency information could be generated. Figure 3-1 provides examples of c(t), m(t), S(t), and their spectra. When f_c and f_m are 40 and 12 Hz, respectively, spectral peaks of S(t) appear at 28 Hz (=(40 – 12) Hz) and 52 Hz (=(40 + 12) Hz).

The lowest light intensity corresponded to the lowest amplitude of the stimulus, and the highest light intensity corresponded to the highest amplitude

by adjusting the DC offset. The continuous amplitude variation of the AM stimulus was digitized in eight bits at 1000 Hz using a microcontroller unit (ATmega128, Atmel, USA), and the stimulus was then converted into an analog signal again to operate the LEDs using a digital-to-analog converter (LTC1657CN, Texas Instrument, USA). Figure 3-1 (e) shows the intensity variation of an LED (solid line) acquired using a photodiode, which has a similar shape as an ideal AM stimulus signal (i.e., S(t), dashed line). Furthermore, its spectrum has the same peak frequencies as those of the ideal AM stimulus signal (Figure 3-1 (f)). The study about AM-SSVEP based BCI was published as a journal paper [47].

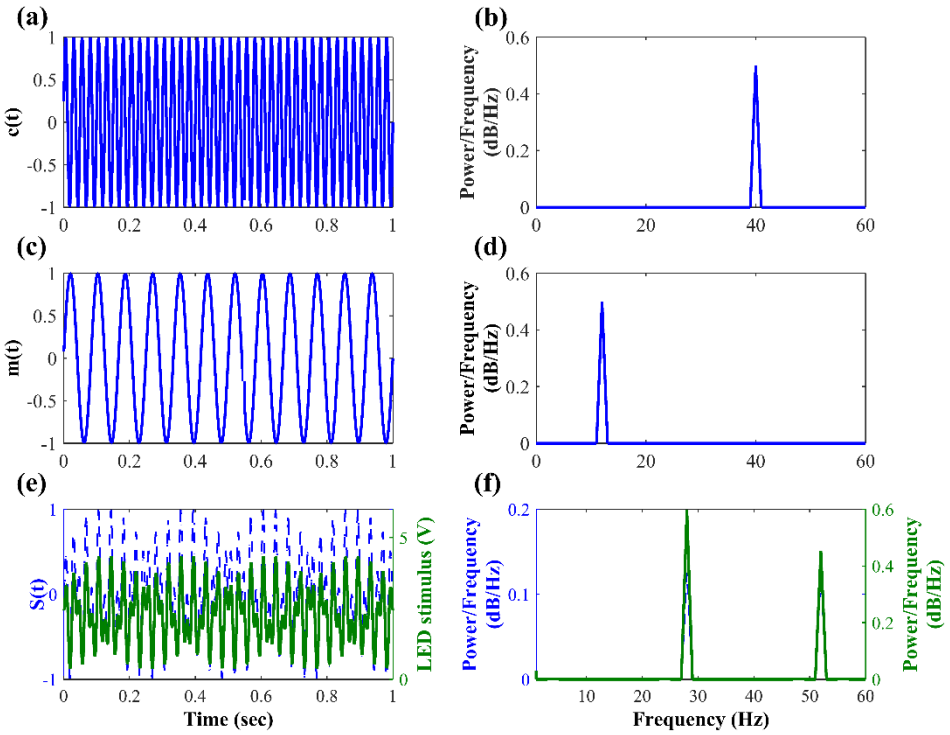

Figure 3-1. Examples of (a) a sine-wave carrier, (c) a sine-wave modulating signal, (e) the AM stimulus, and (b), (d), (f) their respective spectra. In (e) and (f), the dashed line and the solid line represent the ideal AM stimulus signal and the LED stimulus signal, respectively.

3.2. Methods

3.2.1. Subjects and Experimental Settings

A total of 12 subjects (10 males and 2 females) between the ages of 24 and 31 participated in the experiments. The subjects had normal or corrected-to-normal vision and had no experience with epileptic seizures. After being sufficiently informed about the experimental procedures, the subjects consented to participate in the study. All of the subjects performed the offline experiment, and nine of them continued the first online experiment (Online 1). The other three subjects did not participate in Online 1 because of their schedules. Three subjects, who achieved 100% accuracy for each stimulus in Online 1, participated in the second online experiment (Online 2) on a different day.

The EEG signals were acquired using g.USBamp at a sampling rate of 512 Hz. The 15 electrodes were located at O1, Oz, O2, PO3, POz, PO4, P1, Pz, P2, P3, P4, P5, P6, PO7, and PO8 following the extended international 10-20 system, around the occipital region that is known to be involved in the generation of SSVEPs [8]. The ground and reference electrodes were placed at Fpz and A1, respectively. During the measurement, a high-pass filter at 2 Hz, a low-pass filter at 100 Hz, and a notch filter at 60 Hz were applied to every amplifier channel.

The offline experiment and Online 1 were conducted in a quiet and dim room without an electromagnetic shield, and Online 2 was conducted in a generally illuminated office room. The subjects were requested to comfortably

sit ~80 cm away from the visual stimuli. The visual stimulus consisted of two LED arrays (SMD 5050-3, Korea) with a diffusion film such that the subjects perceived it as a large light source. Six visual stimuli (L, UL, U, UR, R, and D) were positioned around an LCD monitor (SyncMaster T260HD, Samsung, Korea; 60-Hz refresh rate) (Figure 3-2).

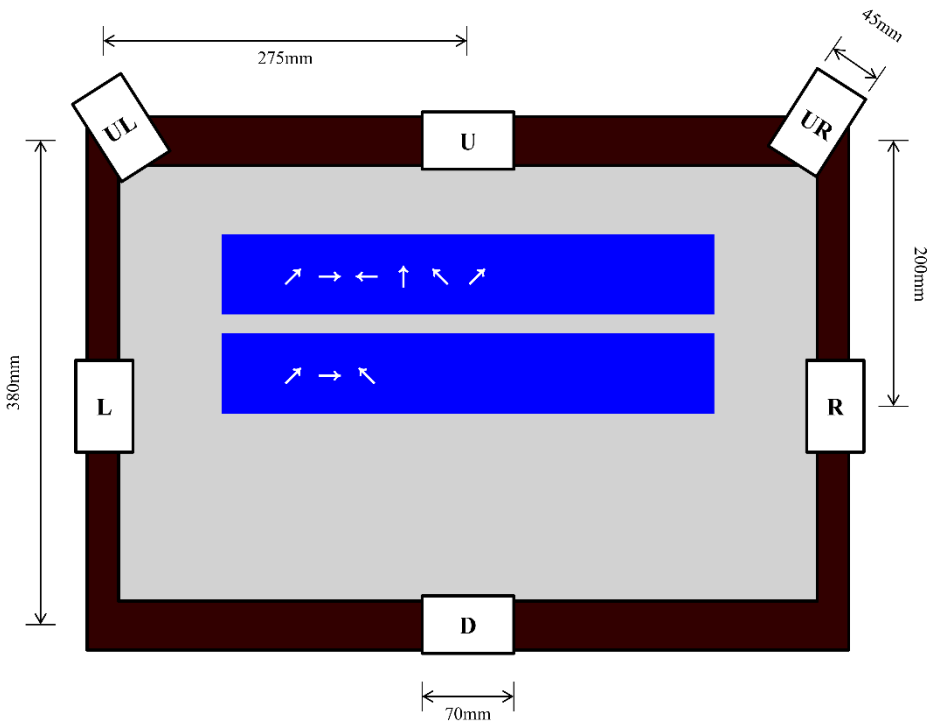

Figure 3-2. Six visual stimuli around a monitor. The tasks where the subjects had to focus are indicated in the center of the monitor by arrows.

3.2.2. Offline Experiments

In the offline experiment, a task involved randomly focusing on one of four targets in the four cardinal directions (L, U, R, and D in Figure 3-2). At the beginning of a trial (t = 0 s), subjects were asked to gaze at the center of a monitor. When an arrow appeared at the center of a monitor at t = 3 s, subjects had to focus on the target where the arrow pointed. To avoid EOG and EMG artifact contamination, we requested that the subjects not blink or move their jaws during this phase [53]. After the arrow disappeared at t = 13 s, the subjects were free to slightly move their eyes or jaws until another arrow appeared. Each trial lasted for 15 s, with 2 s to provide enough time to alleviate eye fatigue after focusing. Only the last 9.5-s segment among the 10-s EEG data was analyzed to exclude noise from eye or head movements during tracking of the target. Four targets (L, U, R, and D) flickered as AM sine waves with different combinations of f_c and f_m (Table 3-1); the f_cs were 40 and 41 Hz in the commonly used high-frequency band [22, 54]; the f_ms were 10, 11, and 12 Hz in the α-band, where the SSVEP amplitude is higher than the amplitude in the high-frequency band [15]. The other two stimuli (UL and UR) were employed in online experiments. A run consisted of 20 trials, and two runs with a 10-min break constituted the offline experiment. Each target was attended equally 10 times.

Table 3-1. Stimulus frequencies of six targets. Four AM stimuli (L, U, R, and D) were used in offline experiments. Six stimuli with three different types of stimulations were used in online experiments.

Stimuli		L	UL	U	UR	R	D
AM	f_c	40	41	41	43	40	40
	f_m	12	12	11	9	11	10
High-frequency		40	41	42	43	44	45
Low-frequency		9	10	11	12	13	14

3.2.3. EEG Analysis

To investigate the frequency characteristics of the EEG responses to the AM stimuli, the power spectral density (PSD) of each target was estimated using the "spectrum" function of g.BSanalyze. The function computed the PSD by detrending and windowing the EEG signal with a "boxcar" window. In the spectra, the signal-to-noise ratio (SNR) of the SSVEP was estimated as the ratio of the Fourier power at a frequency and the average Fourier power at its eight adjacent frequencies [8, 15]. A peak frequency of the SSVEP was defined as that with a SNR higher than 3. Among the peak frequencies, a frequency component commonly observed in more than two spectra, across all of the spectra of the four targets (of all electrodes), was defined as an AM harmonic frequency (f_{AMH}). The canonical correlation between the EEG signal and reference signal of the combination of f_{AMH} was used as a feature for AM-SSVEP recognition.

Frequency recognition of AM-SSVEP was performed using CCA as in 2.2.2. With *N* targets of N different frequencies, *N* different reference signals are required for frequency recognition. Because a traditional visual stimulus flickers at only one frequency, Y_f can be used for traditional SSVEP-based BCI systems. However, an AM stimulus employs more than two flickering frequencies such that at least two Y_f s are required to recognize the brain response to an AM stimulus. In this paper, for simpler AM-SSVEP detection, a novel composition of *Y* was devised. From (10), an AM stimulus can be deemed as the sum of two *sine* waves of $f_c + f_m$ and $f_c - f_m$. However, other f_{AMH}

components may also be helpful for frequency recognition. The novel reference signal, Y_{AM}, was set as the *sine* and *cosine* of a combination of f_{AMH}s and their second harmonics. The combination always included fundamental stimulus frequencies (f_{fund}s; $f_{\mathrm{AMH1}} = f_c + f_m$ and $f_{\mathrm{AMH2}} = f_c - f_m$). Thus, the canonical correlation between the EEG signal and a multi-frequency stimulus can be estimated using only one novel reference signal instead of multiple reference signals. Consequently, AM-SSVEP recognition with multiple peak frequencies was simplified using only one reference signal. The reference signal for the AM stimulus was expressed as

$$Y_{AM} = \begin{pmatrix} \sin(2\pi(f_c + f_m)t) \\ \cos(2\pi(f_c + f_m)t) \\ \sin(4\pi(f_c + f_m)t) \\ \cos(4\pi(f_c + f_m)t) \\ \sin(2\pi(f_c - f_m)t) \\ \cos(2\pi(f_c - f_m)t) \\ \sin(4\pi(f_c - f_m)t) \\ \cos(4\pi(f_c - f_m)t) \\ \sin(2\pi f_{AMH3}t) \\ \cos(2\pi f_{AMH3}t) \\ \sin(4\pi f_{AMH3}t) \\ \cos(4\pi f_{AMH3}t) \\ \vdots \end{pmatrix}. \quad (11)$$

The EEG was finally classified as the conventional CCA in (6).

Every combination of N_{AMH}-AM harmonics (f_{AMH}) was used in the reference signal to find the customized frequency combination (CFC) with the best performance for each subject. As f_{fund}s were always included in the combination, $2^{N_{AMH}-2}$ combinations were tested using four-fold cross

validation. The trials were divided into four equal-sized subgroups. Three subgroups (thirty trials) were used as the training data set, with which the accuracies were estimated for each combination. The best combination was selected as the one with the highest accuracy. The remaining subgroup (ten trials) was the validation data set used for testing the best combination. These steps were repeated until every fold was used as validation data; thus, the four best frequency sets were selected for each training set. Among the four best combinations, the most selected combination was the CFC of a specific window length (i.e., t_w). If two combinations were selected as the best combination, the CFC of t_w was selected as the one with the highest validation accuracy. The window length varied from 1 to 9 s, with intervals of 1 s, and a total segment length of 9.5 s. The accuracy of f_{fund}s across all trials and those of CFCs across the training and validation sets were compared using repeated-measures ANOVA ($\alpha = 0.05$).

3.2.4. Online Experiments

Two online experiments were performed under different conditions: Online 1 was performed directly after the offline experiment under dim light; Online 2 was performed on a different day under general illumination. Online 1 consisted of three types of random six-arrow tasks for each stimulus method, and Online 2 consisted of twenty types of tasks. A task involved typing six arrows using five arrows pointing in different directions (←, ↖, ↑, ↗, and →) and one backspace (BS). Each arrow corresponded to each target in the same

direction (e.g., ← to L) and BS to D. The subjects typed a specific arrow by attending to a pertinent target, and the result of SSVEP recognition was presented in the monitor. If the classification result was "BS," the previous result was removed.

Figure 3-2 illustrates the online environmental setting and an example of a task. The task was shown at the top of the monitor, and the classification results were shown just beneath the task. To complete the task, the subjects had to focus on UR – R – L – U – UL – UR in series without any errors. However, the third arrow (←) was misclassified as the arrow pointing toward the upper left (↖), necessitating a correction. In this case, the subjects had to attend to D to delete the error and again attend to L to type the right answer. The subjects were sufficiently instructed on how to type an arrow and delete an error before starting the online experiments.

Three types of stimulus methods were employed in the online experiments to verify the utility of AM stimuli for the SSVEP-based BCI system: AM, high-frequency, and low-frequency stimuli. The stimulus frequencies for these methods are shown in Table 3-1. For the AM stimuli, f_c and f_m ranged from 40 to 43 Hz and from 9 to 12 Hz, respectively. Compared with the offline experiment, new combinations of f_c and f_m ((41 – 12) Hz for UL and (43 – 9) Hz for UR) were added in the online experiments to evaluate the feasibility of various other combinations. The high-frequency stimuli flickered at 40–45 Hz, and the low-frequency stimuli flickered at 9–14 Hz. These frequencies were near f_cs and f_ms, respectively, and have been used in conventional SSVEP

studies [15, 22, 55]. The experimental procedure was random in both the tasks and stimulus methods. The subjects rested for ~5 min between experiments of different stimulus methods. After all of the procedures of Online 1, the subjects filled out a questionnaire in which they scored the sense of flickering, eye fatigue, and everyday usability of the three stimulus methods on a scale of 1 to 10. As the sense of flickering (how large they sensed the change of light intensity to be) or eye fatigue (to what extent they felt eye fatigue) was weaker, subjects scored lower points for each criterion. Furthermore, the subjects gave higher points if they felt that they could use stimuli such as the SSVEP-based BCI system in their daily life (e.g., simple on/off button on a television). Several studies have tried to quantify the level of eye fatigue using physiological signals, such as eye blink frequency [56], galvanic skin response (GSR), skin temperature (SKT), and EEG [57, 58]. However, the methods have not been examined for SSVEPs in various frequency ranges and have not been standardized. Thus, only subjective evaluation was performed in this study.

The online SSVEP-based BCI system was designed based on a previous study [15]. In this study, new 256-point EEG data were stored in a 4-s-long buffer (data buffer) every 0.5 s. Then, the existing data were shifted, removing the initial 0.5 s of data to generate a new 4-s segment. Until the buffer was full of real EEG data in the first 4 s, it was zero-padded. The SSVEP was recognized with the 4-s EEG signal using the CCA method every 0.5 s. A classified temporal decision from CCA was stored in another buffer (decision buffer). If four consecutive temporal decisions were the same, the corresponding decision

was selected as the final decision and the data buffer was cleared out. If not, after 0.5 s, a new temporal decision was stored in the decision buffer; the temporal decisions shifted, and the first decision was removed; then, four consecutive decisions were compared again. The most rapid final decision could be classified in 2 s (2 s for the same four consecutive temporal decisions).

When CCA was conducted, the reference signals were traditional ones (Y_f s) such as (5) with $N_h = 2$ for high- and low-frequency stimuli. For AM stimuli, Y_{AM}s were used with $N_h = 2$, as in high- or low-frequency stimuli. f_{AMH}s for Y_{AM} were CFC including f_{fund}s from offline analysis, which was the best combination when $t_w = 4$ because the length of the data buffer was 4 s. Thus, Y_{AM} consisted of *sine* and *cosine* of CFC and second harmonics of CFC as in (11). A temporal decision was classified as the one with the highest correlation as in (6).

The accuracy and ITR were estimated as

$$\text{Accuracy} = \frac{N_{correct}}{N_{total}} \tag{12}$$

$$\text{ITR} = \frac{60}{command\ transfer\ interval} \cdot [\log_2 N + p \log_2 p + (1 - p) \log_2 \left(\frac{1-p}{N-1}\right)], \tag{13}$$

where p is the accuracy in (12) and N represents the number of targets ($N = 6$ in this study); the *command transfer interval* is the average time required to complete the tasks for the same stimuli [59, 60]. The performance and scores

in every category of the questionnaire between stimuli were statistically compared using repeated-measures ANOVA ($\alpha = 0.05$).

3.3. Results

3.3.1. Harmonics of AM-SSVEP

After the spectral peak frequencies were arranged for each target, the AM harmonic frequencies were discerned as the same frequency components appearing for each subject. For example, when a spectrum of L peaks at 80 Hz and a spectrum of U peaks at 82 Hz, the $2f_c$ component was defined as f_{AMH} because such frequencies are harmonics of f_c of L and U (40 and 41 Hz; 80 Hz = 40 Hz × 2 and 82 Hz = 41 Hz × 2). However, different components were observed at different electrode channels, with different targets, or for different subjects. Figure 3-3 (a) presents a spectrum of SSVEP measured at O1 when subject 1 (S1) focused on L, where three AM harmonic frequencies occur at $2f_m$ (24 Hz), $f_c - f_m$ (28 Hz), and $2f_c - 4f_m$ (32 Hz). However, the $2f_m$ component did not appear in the spectra of the SSVEP at a different electrode (O2, Figure 3-3 (b)). When the same subject focused on a different target (D), a $f_c + f_m$ (50 Hz) component of SSVEP newly appeared at the same electrode (O1, Figure 3-3(c)). For subject 6 (S6, Figure 3-3 (d)), spectral peaks at $f_c - 3f_m$ (4 Hz) and $f_c + f_m$ (52 Hz) occurred and a peak at $2f_c - 4f_m$ (32 Hz) did not occur compared with those of S1 with the same target and electrode position (Figure 3-3 (b)). Second or third harmonics of AM harmonic frequencies sometimes occurred.

From the spectra of all of the subjects, a total of seven different AM harmonic frequencies were observed: $2f_c$, $2f_m$, $f_c \pm f_m$, $f_c \pm 3f_m$, and $2f_c - 4f_m$. Table 3-2 shows f_{AMH} observed in offline analysis for L, U, R, and D and the estimated f_{AMH} for the other stimuli additionally used in the online experiments

(UL and UR). While the stimulus frequencies were approximately 10 Hz for f_ms and 40 Hz for f_cs, spectral peaks occurred in a wide frequency range from less than 10 Hz to more than 80 Hz except for at ~60 Hz because of a notch filter. This range covered both low- and high-frequency bands in a conventional SSVEP-based BCI system. Every combination of the harmonic frequencies was tested with 4-s EEG signals to determine the best one for each subject, which was used in the online experiments.

Table 3-2. AM harmonic frequency components and their frequency values

f_{AMH}	L	UL	U	UR	R	D
$2f_c$	80	82	82	86	80	80
$2f_m$	24	24	22	18	22	20
$f_c - f_m$	28	29	30	34	29	30
$f_c + f_m$	52	53	52	52	51	50
$f_c - 3f_m$	4	5	8	16	7	10
$f_c + 3f_m$	76	77	74	70	73	70
$2f_c - 4f_m$	32	34	38	38	36	40

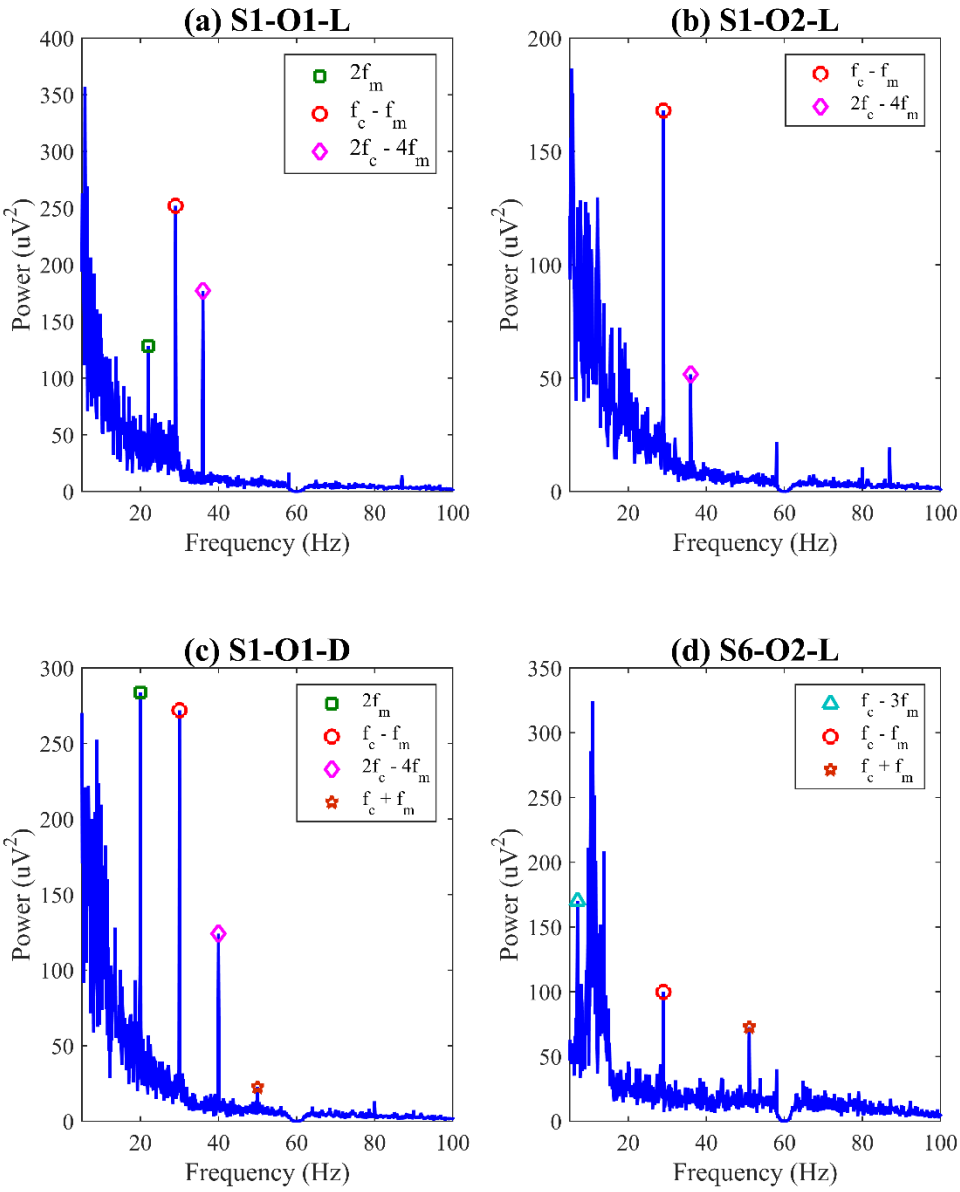

Figure 3-3. The spectra of 9.5-s-long SSVEPs and different types of AM harmonic frequencies measured at (a) O1 when S1 focused on L, (b) O2 when S1 focused on L, (c) O1 when S1 focused on D, and (d) O2 when S6 focused on L.

3.3.2. Offline Analysis

As t_w increased from 1 to 9.5 s, ten different CFCs were selected in terms of the accuracies of training and validation sets. The CFCs could coincide with those of different t_w, and this trend was more frequently observed as t_w increased. A combination of more frequency components did not always perform better than that of less frequency components. The training and validation accuracies were averaged over folds of the same t_w, where the relevant CFC had the highest accuracy. The average accuracies across all of the subjects are shown in Figure 3-4 (a). The solid line and the dashed line represent the accuracies of the CFCs with training data and validation data, respectively. The dotted line represents global accuracies when only f_{AMH} composed f_{fund}s in (11). The accuracies were significantly different with window length t_w ($F(9, 25) = 48.534$, $p < 0.001$) and conditions (training, validation, and fundamental stimulus frequencies in Figure 3-4 (a); $F(18, 50) = 2.129$, $p < 0.05$). Tukey's honestly significant difference (HSD) test suggested that CFC was superior to f_{fund} for SSVEP classification; the average accuracies of the training and validation sets were 93.1 ± 13.4% and 91.7 ± 15.5%, respectively, and the total accuracy of f_{fund}s was 81.4 ± 16.8%. Examples of the CCA weights distribution and the PSD of a canonical variant are presented in Figure 3-4 (b) and (c). Both the CCA weights and spectrum were estimated with 15-channel 9-s SSVEPs acquired when S1 focused on D. In the CCA weights scalp distribution (Figure 3-4 (b)), the highest positive coefficient is with Oz and the lowest negative one is with Pz. In the PSD of a

canonical variant (i.e., *x*; Figure 3-4 (c)), dominant peaks appear at two more f_{AMH}s compared with those of raw EEG data in Figure 3-3 (c).

.

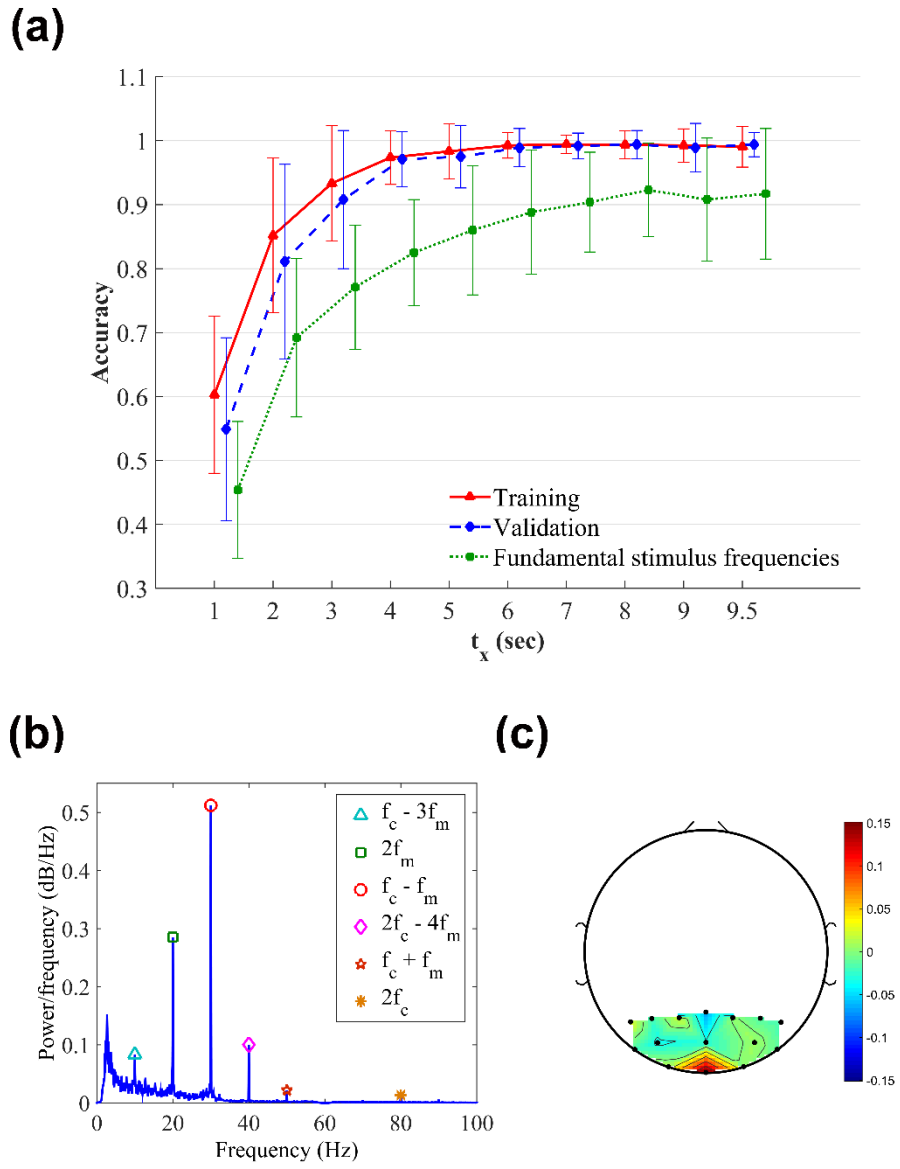

Figure 3-4. (a) Accuracies of training and validation sets with CFCs and global accuracy with f_{fund} according to t_w (mean ± SD). Examples of (b) CCA coefficient scalp distribution with the highest correlation and (c) PSD of the relevant canonical variant.

3.3.3. CFC for Online Analysis

The composition of Y_{AM} should be the best combination for the online experiment of AM stimuli, as appropriate feedback should be given to the subjects. Online frequency recognition was performed on 4-s-long EEG data; thus, a CFC of a 4-s window length in offline analysis was used for Y_{AM}. The combination always included f_{fund}s, even if they were not peak frequencies. Table 3-3 lists the peak frequencies in the spectra of 4-s EEG signals, defined as f_{AMH}, and the CFCs for online experiments of each subject. Notably, the spectral peak frequencies were not always equal to the best "features." For example, peaks occurred at $2f_c - 4f_m$ for the spectra of S2; however, this peak was not included in CFC. In contrast, $f_c + 3f_m$ performed an important role in SSVEP classification, even if the component was not dominant in the SSVEP of S2.

Table 3-3. Spectral peak frequencies of 4-s EEG signals and CFCs for online experiments. Subjects whose CFCs are blank did not participate in online experiments.

Subjects	Spectral peaks	Customized Frequency Combination
1	$f_c - f_m$, $2f_m$, $2f_c - 4f_m$	$f_c \pm f_m$, $2f_m$, $2f_c - 4f_m$
2	$f_c - f_m$, $2f_m$, $2f_c - 4f_m$	$f_c \pm f_m$, $f_c + 3f_m$, $2f_m$
3	$f_c - f_m$, $2f_c - 4f_m$	-
4	$f_c - f_m$, $2f_m$, $2f_c - 4f_m$	$f_c \pm f_m$, $2f_m$
5	$f_c - f_m$, $2f_m$	$f_c \pm f_m$, $2f_m$, $2f_c - 4f_m$
6	$f_c - f_m$	-
7	$f_c - f_m$	$f_c \pm f_m$, $2f_m$
8	$f_c \pm f_m$	-
9	$f_c - f_m$, $2f_c - 4f_m$	$f_c \pm f_m$, $2f_c - 4f_m$
10	$f_c - f_m$	$f_c \pm f_m$, $2f_m$
11	$f_c - f_m$, $2f_m$, $f_c - 3f_m$	$f_c \pm f_m$, $2f_m$
12	$f_c - f_m$, $2f_c - 4f_m$	$f_c \pm f_m$, $2f_m$, $2f_c$, $2f_c - 4f_m$

3.3.4. Online Analysis

Figure 3-5 illustrates the online classification process for a task. The dash-dot line indicates a series of targets where a subject had to attend. The dashed line shows the change in temporal decision, which changes every 0.5 s. The solid line denotes the change in final decision that was regarded as the target to which a subject attended. At first, 0.5 s was required to store an EEG signal in a buffer; up to a 0.5-s temporal decision, the final decision was "None." At 0.5 s, the temporal decision on the first 0.5 s data was classified as R, even though the target was U. At 2 s, temporal decisions changed from R to L. However, the four temporal decisions did not remain the same; therefore, the final decision was still "None." From 2.5 s, the other four consecutive temporal decisions were identical to U, resulting in the first final decision as U at 4 s. Because the final decision was the same as the target, the next target was transformed into UL. In total, 4 s was required to classify the first command. However, the fifth target was rapidly classified because the first four temporal decisions were the same as the target, L. Because no error occurred in this example, BS (D) was not assigned as a target.

All of the input results were recorded with respect to the tasks, stimuli, and subjects to estimate accuracies. The number of inputs including the wrong inputs and BS was considered to estimate the performance indices. The average accuracies and ITRs in Online 1 were estimated according to the stimuli and subjects (Table 3-4). Among the three stimuli, the AM stimuli outperformed the high- or low-frequency stimuli in terms of both accuracy and ITR. However,

this difference was not significant ($F(2, 16) = 0.906$, $p > 0.424$ for accuracy, and $F(2, 16) = 0.109$, $p > 0.897$ for ITR). In contrast, the BCI performance in Online 2 was the highest with the low-frequency SSVEP (Table 3-5). The difference in accuracies was not significant ($F(2, 114) = 2.726$, $p = 0.070$); however, the difference in ITRs was significant ($F(2, 114) = 7.139$, $p = 0.01$) and depended on the subjects ($F(4, 114) = 3.151$, $p = 0.017$). The ITR of the low-frequency SSVEP was significantly different than the high-frequency and AM- SSVEPs ($p = 0.01$ for AM-SSVEP; $p = 0.004$ for high-frequency SSVEP).

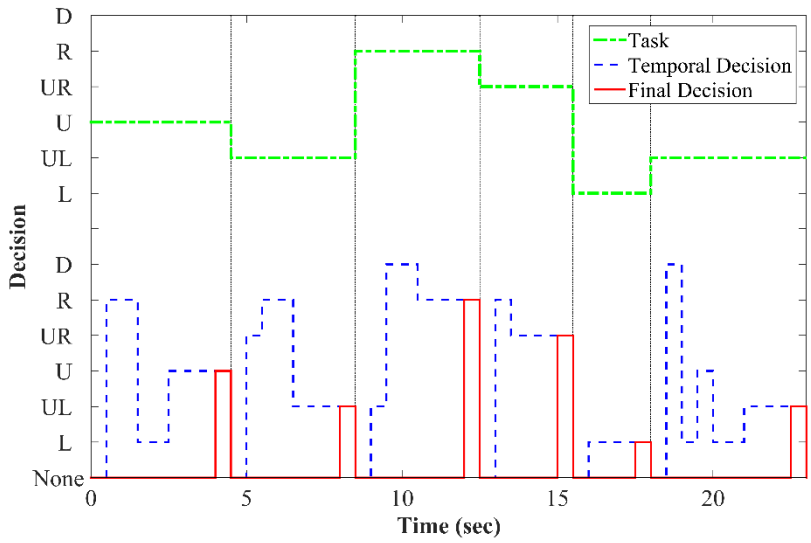

Figure 3-5. Online classification diagram when subject 5 (S5) performed a third task with AM stimuli.

Table 3-4. Performance indices of three types of stimuli for Online 1

Subjects	AM-SSVEP				High-frequency SSVEP				Low-frequency SSVEP			
	$N_{correct}/N_{total}$	T_{total} (s)	Accuracy (%)	ITR (bit/min)	$N_{correct}/N_{total}$	T_{total} (s)	Accuracy (%)	ITR (bit/min)	$N_{correct}/N_{total}$	T_{total} (s)	Accuracy (%)	ITR (bit/min)
1	6/6	23.5	100.0	41.7	7/8	29.5	90.9	29.5	7/8	30.5	87.5	27.3
	6/6	23.5			6/6	23.5			8/10	38.5		
	6/6	20.0			7/8	33.5			6/6	23.5		
2	8/10	40.0	87.5	27.3	8/10	38.5	87.5	26.7	7/8	28.0	95.0	37.1
	7/8	30.5			6/6	21.0			6/6	21.5		
	6/6	22.0			7/8	35.0			6/6	21.0		
4	7/8	28.0	95.0	34.5	7/8	27.0	78.1	21.6	6/6	20.0	72.5	19.7
	6/6	22.5			11/16	59.0			12/16	47.0		
	6/6	25.5			7/8	31.0			13/20	66.5		
5	7/8	27.5	90.9	31.1	6/6	23.5	87.5	29.3	6/6	24.0	100.0	42.3
	7/8	32.0			6/6	21.5			6/6	21.0		
	6/6	22.5			9/12	41.0			6/6	21.0		
7	10/14	61.5	72.5	14.6	6/6	25.5	84.6	25.0	9/12	44.5	73.7	17.6
	9/12	62.5			9/12	47.5			11/16	61.0		
	10/14	56.0			7/8	27.5			8/10	42.5		
9	7/8	40.5	87.0	22.4	6/6	24.0	95.0	35.2	6/6	24.5	87.5	26.4
	8/10	46.5			6/6	23.0			8/10	38.0		
	6/6	25.5			7/8	27.5			7/8	33.0		
10	6/6	20.0	100.0	40.2	6/6	20.5	78.1	20.1	8/10	35.0	78.1	22.3
	6/6	23.5			9/12	52.0			6/6	20.5		
	6/6	26.0			10/14	53.5			11/16	58.0		
11	6/6	24.0	100.0	38.8	6/6	21.0	100	43.3	6/6	22.5	95.0	35.9
	6/6	23.5			6/6	21.5			7/8	27.5		
	6/6	24.5			6/6	22.0			6/6	23.0		
12	7/8	35.5	87.5	23.2	7/8	30.0	90.9	30.0	7/8	29.0	90.9	32.9
	8/10	46.0			7/8	30.0			7/8	28.5		
	6/6	27.0			6/6	25.0			6/6	20.0		
Average			91.2	30.4			88.1	29.0			86.7	29.1

Table 3-5. Performance indices of three types of stimuli for Online 2

Subjects	AM-SSVEP		High-frequency SSVEP		Low-frequency SSVEP	
	Accuracy (%)	ITR (bit/min)	Accuracy (%)	ITR (bit/min)	Accuracy (%)	ITR (bit/min)
1	97.13	42.87	91.55	35.40	96.25	43.08
5	96.79	40.24	97.50	38.69	97.95	44.25
11	97.13	35.13	95.79	40.41	98.75	43.21
Average	97.02	39.41	94.95	38.17	97.65	43.51

3.3.5. Subject Evaluation

The subjects participating in Online 1 evaluated eye fatigue, the sense of flickering, and the feasibility of daily use with respect to three types of stimuli (Figure 3-6). For each category, the scores were different based on the stimulus types ($F(2, 24) = 7.330$, $p < 0.01$ for eye fatigue, $F(2, 24) = 56.492$, $p < 0.001$ for sense of flickering, and $F(2, 24) = 18.984$, $p < 0.001$ for daily use). From post-hoc analysis using Tukey's HSD test, the low-frequency SSVEP was confirmed to have yielded higher scores than the others in the eye fatigue category (7.56 ± 3.13 points; $p < 0.05$ between low- and high-frequency stimuli, and $p < 0.01$ between low-frequency and AM stimuli) and in the sense of flickering category (9.00 ± 1.00 points; $p < 0.001$). In the daily use category, the low-frequency stimuli received a lower score than the other two stimulus types (3.11 ± 1.69 points; $p < 0.001$). In other words, low-frequency stimuli caused much higher eye fatigue and sense of flickering than high-frequency and AM stimuli. Furthermore, the subjects regarded AM and high-frequency stimuli to be more suitable for use in daily life than low-frequency stimuli.

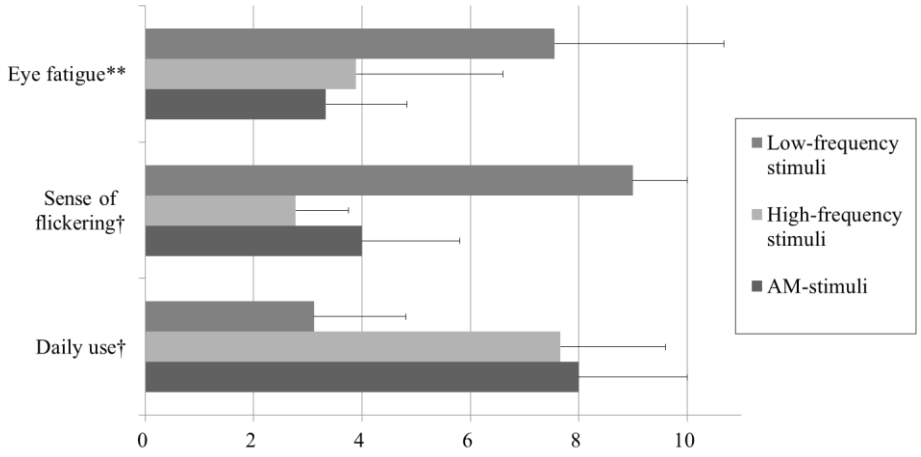

Figure 3-6. Subject evaluation with standard deviation in terms of eye fatigue, sense of flickering, and the feasibility of daily use according to the visual stimulus types (mean ± SD). $^{**}p < 0.01$, $^{\dagger}p < 0.001$.

3.4. Discussion

3.4.1. Combining of Low- and High-Frequency SSVEPs

In this section, the SSVEP response evoked by an AM stimulus was investigated and verified its availability in a SSVEP-based BCI system with low eye fatigue. The AM stimulus was devised to deliver low-frequency information carried in a high-frequency stimulus, resulting in multi-frequency stimulation. In this experiment, the carrier frequencies were higher than 40 Hz and the modulation frequencies were ~10 Hz, which allowed actual flickering frequencies ($f_c \pm f_m$) higher than 30 Hz. We employed such frequency combinations for two reasons. First, the combinations increased the actual flickering frequencies and therefore permitted a reduction in eye fatigue. Because the SNR decreases in the high-frequency band [18], the actual flickering frequencies were adjusted so as not to exceed 55 Hz. If both the carrier and the modulation frequencies were above 30 Hz, one of the actual stimulus frequencies, i.e., $f_c - f_m$, would be in the low-frequency band. Then, the low-stimulus frequency would cause more eye fatigue, and other increased harmonic frequencies would have much lower SNRs. Another reason for the use of such combinations was to utilize low-frequency harmonic information under 30 Hz. As mentioned earlier, the SSVEP power in the low-frequency band is larger than that in the high-frequency band, and many research groups have exploited this fact. Similarly, the low-frequency information ($2f_m$) actually played an important role in AM-SSVEP recognition (Table 3-3).

With an optimized combination of frequencies, the AM-SSVEP produced higher or equivalent accuracy as the low-frequency SSVEP and higher accuracy and ITR than the high-frequency SSVEP. Eye fatigue with AM stimuli was lower than that with high-frequency stimuli by 0.55 points despite a higher sense of flickering by 1.22 points. Considering the performance and subject evaluation, AM-SSVEP appears to be more feasible than the other stimuli for use in daily life, as evaluated by the subjects.

High BCI performance and the evaluation results with AM-SSVEP might arise from the good aspects of low- and high-frequency SSVEPs—the high amplitude of low-frequency SSVEP and low eye fatigue of high-frequency SSVEP. Spectral analysis demonstrated the effect of low-frequency SSVEPs in power difference using the Kruskal-Wallis test ($p < 0.001$, Table 3-6). The power at $f_c - f_m$ was the largest, followed by that at $f_c - 3f_m$ and $2f_m$, all of which are in the low-frequency band that is well known for having large amplitude. The largest power at $f_c - f_m$ most likely arose because it was one of the actual stimulus frequencies (f_{fund}). The large powers at $f_c - 3f_m$ and $2f_m$ might be observed because they are in the low-frequency band [15]. In addition, the $2f_m$ component was employed in AM-SSVEP recognition for most of the subjects. The characteristics of the SSVEP response to a low-frequency stimulus seemed to be observed in those of the AM-SSVEP. This phenomenon was unexpected outcome because the real stimuli did not flicker at such low frequencies. However, it has not been proved yet that the low-frequency-like performance came from the non-linear processing in the brain as if AM stimulus contained

low-frequency information. Meanwhile, the AM stimulus was considered to cause the least eye fatigue and to be the most feasible in daily life from the subject evaluation. The evaluation results are similar to those of the high-frequency stimulus, suggesting that the AM stimulus benefits from the advantages of high-frequency stimuli.

Table 3-6. Average spectral power and SNR at f_{AMH}

f_{AMH}	Power (uV^2)					SNR				
	L	U	R	D	Average	L	U	R	D	Average
$f_c - f_m$	229.40	207.86	273.61	260.47	242.84	6.65	6.34	7.27	6.85	6.78
$f_c + f_m$	17.10	20.62	17.28	19.10	18.53	1.58	1.76	1.67	2.20	1.80
$f_c - 3f_m$	203.33	159.51	106.38	237.09	176.58	1.26	1.76	1.17	1.60	1.45
$f_c + 3f_m$	7.40	8.94	8.12	9.32	8.44	0.91	1.09	0.94	1.26	1.05
$2f_c$	9.72	8.98	9.75	9.17	9.40	1.27	1.30	1.44	1.46	1.37
$2f_m$	62.04	91.30	88.15	112.47	88.49	2.36	2.65	2.56	3.07	2.66
$2f_c - 4f_m$	31.91	37.78	32.72	31.67	33.52	1.84	2.50	2.22	2.63	2.30

3.4.2. AM Harmonic Frequencies in CFC

f_{AHM} ranged from the very low-frequency band under 6 Hz to the relatively high-frequency band above 70 Hz. However, not all of the f_{AMH}s appeared simultaneously in the AM-SSVEPs, as demonstrated in Figure 3-3. Therefore, we extracted the CFC from each subject's visual response. Most CFCs included $2f_m$ and $2f_c - 4f_m$ components, which were not always identical to the spectral peaks (Table 3-3). Therefore, we analyzed the characteristics of the elements of the CFCs in terms of power and SNR (Table 3-6). The spectral power of the low-frequency band was much higher than that of the high-frequency band, as mentioned above: at $f_c - f_m$, $f_c - 3f_m$, and $2f_m$. The SNR also differed significantly depending on f_{AHM} ($p < 0.001$, Table 3-6). The three largest SNRs were those at $f_c - f_m$, $2f_m$, and $2f_c - 4f_m$. Because $f_c - f_m$ was always included in the CFC, we further considered only the three f_{AMH}s that had large power or SNR: $2f_m$, $f_c - 3f_m$, and $2f_c - 4f_m$. The three f_{AMH}s represented three groups: (1) one with high power and high SNR ($2f_m$), (2) one with low power and high SNR ($2f_c - 4f_m$), and (3) one with high power and low SNR ($f_c - 3f_m$). The $2f_m$ component with both high power and high SNR was included in the CFCs of most subjects (Table 3-3). The $2f_c - 4f_m$ component with high SNR and low power was selected as an important feature for approximately half of the subjects (4/9) despite its low power. However, the $f_c - 3f_m$ component was never selected as the CFCs for frequency recognition even with high power. Thus, we could infer that the f_{AMH} with both high power and high SNR is the best component for

frequency recognition of AM-SSVEPs. Furthermore, the frequencies with high SNR are more important for Y_{AM} than those with high power.

3.4.3. Error Analysis

Error analysis was performed using data from the offline experiment with four targets. We assumed that EEG signals longer than 4 s would be suitable for reliable BCIs with the best accuracies higher than 95%; therefore, the data of 4 s and above were used for error analysis. Figure 3-7 presents the confusion matrix for the presented targets and the classified targets. The error rates of U and D were high and were mostly misclassified as each other. This phenomenon may arise from the use of the same fundamental frequency ($f_c - f_m$) because such a frequency had the highest SNR for both targets (Table 3-6). Because the SNR determines the relative importance of harmonic frequencies in SSVEP recognition, the same fundamental frequencies with the highest SNR may be confused for one another. However, the error rate of ~5% between U and D is relatively low, even with the same stimulus frequency. Such low false positive rates of AM-SSVEP may be due to the use of non-integer harmonic components for SSVEP recognition. If the fundamental stimulus frequencies overlap in conventional SSVEP-BCI systems, they can never be distinguished from each other. In terms of multiple harmonics, more than 16% of the targets were misclassified as their sub-harmonic frequencies using conventional CCA [51]. The possibility of using the same frequencies is an advantage of AM-SSVEP,

which would enable the generation of more targets through the combination of a few frequencies.

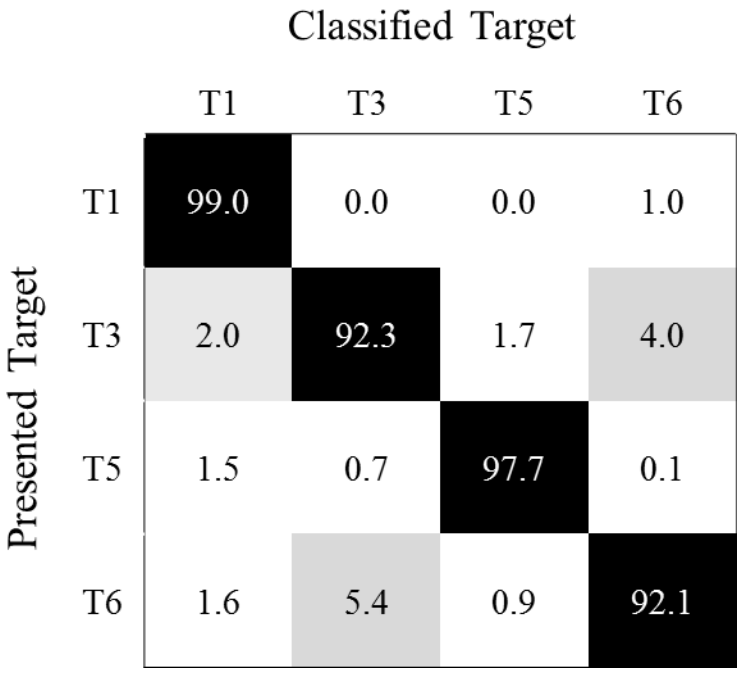

Figure 3-7. Confusion matrix for the offline experiment data. Each value indicates the true positive rates (%) in the diagonal row and the false positive rates (%) in the others.

3.4.4. Effects of Environmental Illumination

In [22], both the accuracy and the ITR of the low-frequency SSVEP were higher than those of the high-frequency SSVEP in a general fair environment. However, although the ITR exhibited the same trend in this study, the accuracy of the high-frequency SSVEP was higher than that of the low-frequency SSVEP in Online 1. The previous trend of BCI performance was not observed in our results, and we deduced that the similar BCI performance of both SSVEPs might result from the dimly illuminated environment. In a dark room, distracting objects can be difficult to perceive and flicker can be more pronounced. Moreover, other external flickering sources cannot affect the visual responses in a dark background. These effects can help subjects to concentrate more on the flicker stimuli rather than on other objects, leading to improvement of SSVEP-based BCI performance [44]. For example, five subjects who had trouble with spelling using an SSVEP-based BCI system put an overcoat over their heads to block background light [61]. Eliminating the background light seemed to reduce frequent errors in the BCI speller system. Three of these subjects reported an improvement in spelling efficacy, and the other two reported that eliminating the background light was effective. In our results, high-frequency SSVEPs seemed to benefit more from these effects.

An additional online experiment (Online 2) was designed to demonstrate the BCI performance of the AM-SSVEP even in an office environment with general illumination compared with Online 1. The results indicated that the low-frequency SSVEP was better than the high-frequency SSVEP, as

demonstrated in previous studies, and that the AM-SSVEP was superior to the high-frequency SSVEP in a general environment (Table 3-5). This result appears to indicate that AM-SSVEP would outperform high-frequency SSVEP even with low eye fatigue under general and dim illumination. However, the experimental conditions were different for Online 1 and Online 2 because these experiments were performed on different days. Thus, the results of Online 2 cannot confirm whether our hypothesis is true: the high-frequency SSVEP benefited more from darkness than the low-frequency SSVEP.

3.5. Conclusion

An AM stimulus delivers low-frequency information carried on a high-frequency carrier, enabling a high-frequency stimulus with low eye fatigue. This stimulus contains several harmonic frequencies in the low- and high-frequency bands, which contributed to BCI performance improvements as classification features. Combinations of a few frequencies generate more targets, and the performance with overlapped stimulus frequencies does not deteriorate performance as much as conventional SSVEP-based BCIs. Thus, people who have a risk of photosensitive epilepsy can substitute a low-frequency stimulus with an AM stimulus without any accuracy deterioration in the BCI system.

The future development of EEG-based BCIs should center on the user for a reliable translation of the brain signal into actions [62]. A reliable BCI system can be achieved with low-cost and convenient equipment (e.g., amplifier, electrodes), good signal processing techniques (e.g., pre-processing, feature extraction, and classification methods), and other application strategies (e.g., stimuli, feedback). Many signal processing algorithms have been devised and optimized for various modalities [5, 21, 51, 63, 64]. With respect to sensing issues, dry EEG electrodes that do not need conductive gel have been recently introduced. Foam-based capacitive electrodes [65] can be used to acquire EEG signals on hair, and a low-cost flexible passive bristle-sensor [66] can produce high-quality EEG recordings with great comfort. For SSVEP application, high-frequency SSVEP [20, 54] and half-field stimulation patterns [37] were

suggested to reduce eye fatigue and the risk of seizure. However, as stated earlier, the high-frequency SSVEP produced worse BCI performance than the conventional low-frequency SSVEP [22], and the average performance of half-field stimuli was comparable or worse than that of a low-frequency stimulus even with a lower chance level [17].

The AM-SSVEP performed well with low-stimulus flashing, demonstrating competitive BCI performance. In addition, a subjective evaluation indicated the suitability of the AM-SSVEP for daily use. Thus, the AM-SSVEP may contribute to the realization of a reliable and nonintrusive SSVEP-based BCI system for the user, which would be more powerful if the AM-SSVEP is integrated with signal processing techniques and more convenient equipment.

4

DFSSVEP-based Hybrid BCI for Improving Classification Rate

4.1. Basic Concepts

The hybrid speller was designed to generate P300 potential and SSVEP simultaneously without interference. In particular, a black-and-white flickering stimulus includes four different characters, which appear periodically in a random sequence. The flickering stimulus and periodic change of the character evokes dual-frequency SSVEP, while the oddball stimulus of the target character evokes P300. The dual-frequency SSVEP peaks at a linear combination of the flickering frequency (SSVEP stimulation frequency) and the frequency of characters appearing (P300 stimulation frequency) rather than the harmonics of the flickering frequency. This approach enables the use of the harmonic SSVEP frequencies for different stimuli in conjunction with relatively prime P300 stimulation frequencies.

The four different characters appear in different colors and places for improved recognition and performance (Figure 4-1 (a)). Thus, nine stimuli consist of 36 characters (A to Z, 1 to 9, and Backspace) arranged in sequence (Figure 4-1 (b)). Each stimulus flickers in black (OFF) and white (ON) with a different flickering period (SSVEP stimulation period; Table 4-1) to evoke SSVEPs. The duty rate remains at 0.8. When the stimulus is ON, one of the four characters appears randomly. The period in the ON state during which a character appears (P300 stimulation period) varies with the stimulus (Table 4-1). For example, a character among A to D appears at every two ON states. Figure 4-2 describes the hybrid speller paradigm for frames 1 to 60. The stimulation frequency is estimated as the *refresh rate*/*stimulation period* (in this study, *120*/*stimulation period*). P300 stimuli (i.e., characters) are presented on the basis of the SSVEP stimulus; thus, the P300 stimulation frequency is sub-harmonic of the SSVEP stimulation frequency. The study about the hybrid SSVEP-P300 BCI was published as a journal paper [67].

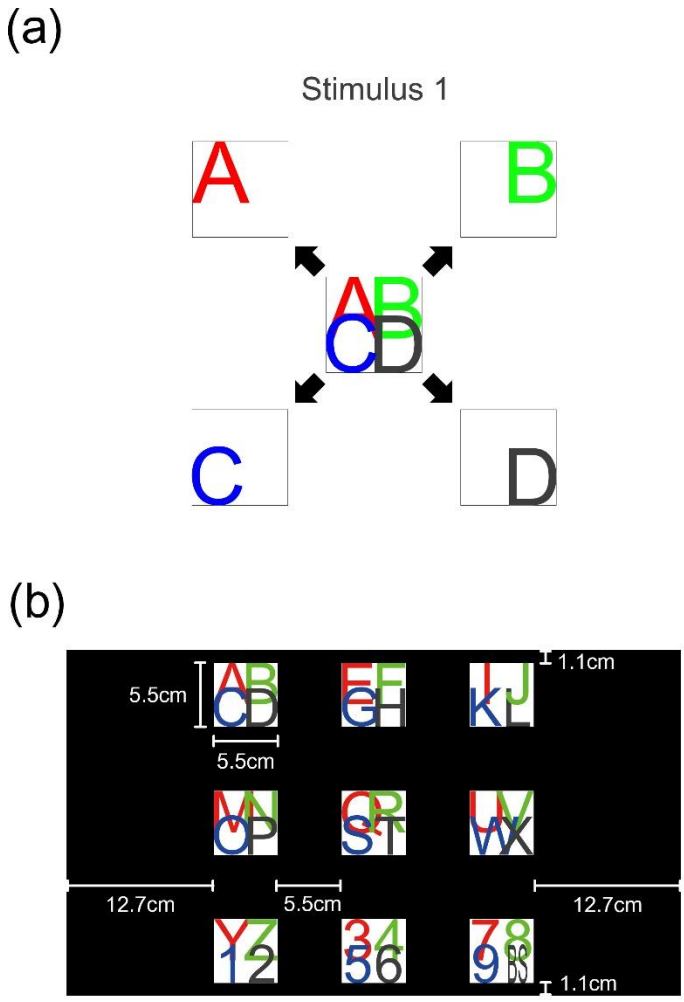

Figure 4-1. Proposed hybrid speller: (a) Composition of the hybrid stimulus and (b) hybrid speller

Table 4-1. Stimulation parameters of the hybrid speller

Stimulus	SSVEP stimulation period	SSVEP stimulation frequency (Hz)	P300 stimulation period	P300 stimulation frequency (Hz)	Flash duration (ms)	SOA (ms)	Stimulation time of a sequence (ms)
1	10	12.0	2	6.0	66.7	166.7	667
2	7	17.1	3	5.7	46.7	175.0	700
3	11	10.9	2	5.5	73.3	183.3	733
4	23	5.2	1	5.2	153.3	191.7	767
5	12	10.0	2	5.0	80.0	200.0	800
6	5	24.0	5	4.8	33.3	208.3	833
7	13	9.2	2	4.6	86.7	216.7	867
8	9	13.3	3	4.4	60.0	225.0	900
9	14	8.6	2	4.3	93.3	233.3	933

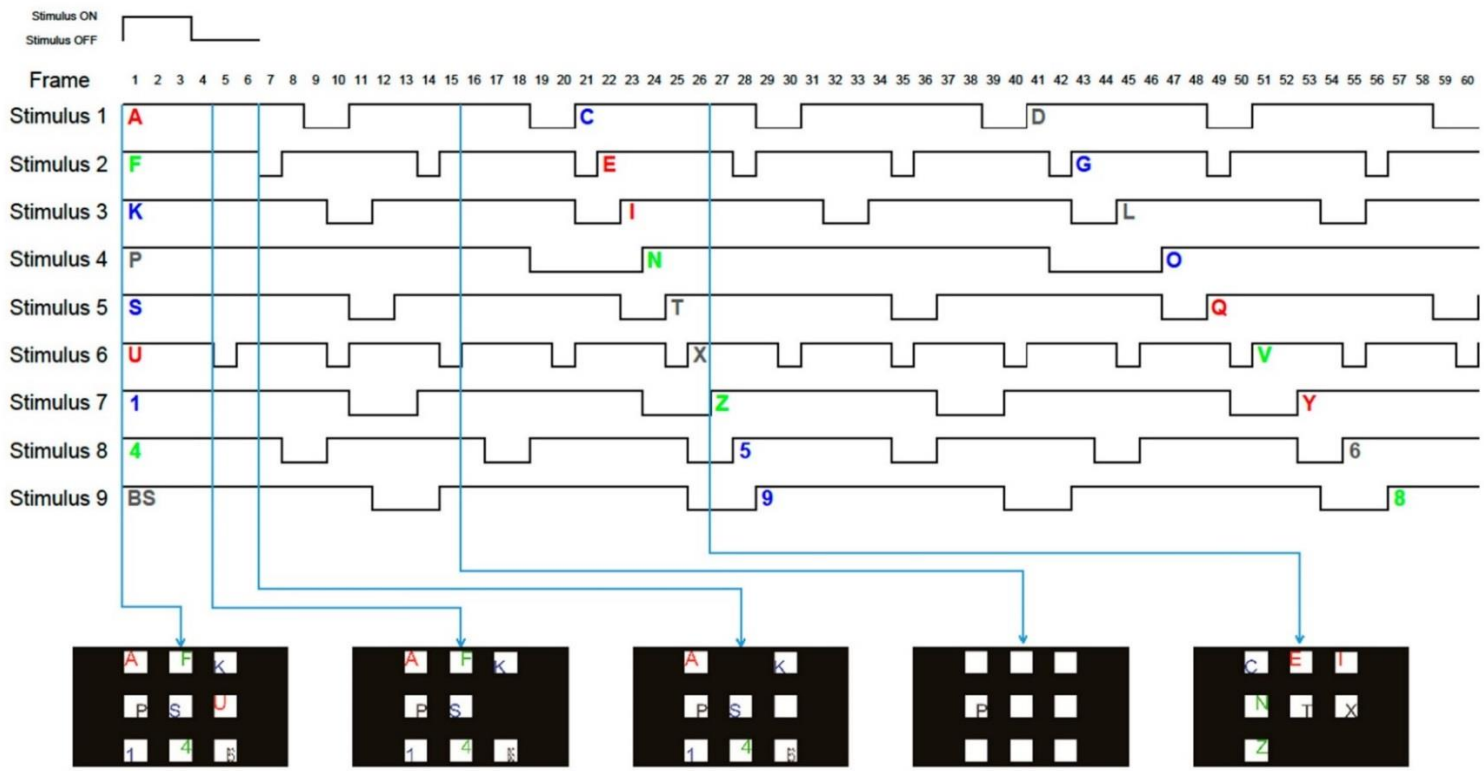

Figure 4-2. Paradigm of the hybrid speller

Each stimulus has a different SSVEP and P300 stimulation period; thus, each stimulus has different P300 stimulation parameters, such as flash duration, stimulus onset asynchrony (SOA: onset-to-onset time), and sequence stimulation time (Table 4-1). In particular, because the stimulation time of a sequence varies with the stimulus, stimulations finish at different times.

$$Stimulation\ time\ (\mathrm{s}) = \frac{SSVEP\ period \times P300\ period}{frame\ rate} \times the\ number\ of\ characters \tag{14}$$

However, the SSVEP response to a stimulus with a short stimulation time has a disadvantage in the SSVEP analysis as compared to that with a long stimulation time. To equalize the SSVEP stimulation time, a stimulus keeps flickering without showing characters after its P300 stimulation time until the last stimulus finishes. The SSVEP response was segmented and analyzed on the basis of the longest stimulation time (i.e., 0.933 s × # sequence, stimulation time of Stimulus 9).

4.2. Methods

4.2.1. Experimental Setting

Ten graduate students (male:female, 8:2; age range, 26.7 ± 2.6 years) participated in the experiments with informed consent. EEG signals were acquired using a g.USBamp with a sampling rate of 600 Hz. Every channel was high-pass-filtered at 0.1 Hz, low-pass-filtered at 60 Hz, and notch-filtered at 60 Hz. Electrodes were placed at 14 channels following the international 10-20 system, namely F3, Fz, F4, Cz, P7, P3, Pz, P4, P8, PO7, PO8, O1, Oz, and O2, on the subjects, grounded at Fpz, and referenced at A1. In the P300 recognition step, a stepwise linear discriminant analysis (SWLDA) automatically chooses channels on the basis of their statistical significance. In the SSVEP recognition step, three electrode configurations were compared in an offline analysis:

Channel Set 1: All 14 channels

Channel Set 2: Oz, PO7, PO8, O1, and O2

Channel Set 3: Oz, PO7, PO8, O1, O2, Pz, P3, P4, P7, and P8

The configuration with the highest accuracy was subsequently used in the online experiments.

The hybrid speller consisted of nine stimuli flickering at different frequencies (Table 4-1). Two pairs of stimuli flickered at harmonic frequencies: Stimuli 1 (120/10 Hz) and 6 (120/5 Hz), and Stimuli 2 (120/7 Hz) and 9 (120/14 Hz). Conventional SSVEP and P300 spellers were employed with equivalent

settings to compare and assess the practicality of the hybrid speller. However, because single-frequency SSVEP-based BCI systems cannot accurately classify SSVEP responses to stimuli that flicker at harmonic frequencies, only seven stimuli were used for the SSVEP speller in the study (Stimuli 3 to 9; Figure 4-3 (a)). The stimuli were represented by a colored number from 3 to 9, where the colors were the same as those of the hybrid stimuli. Both the hybrid speller and the SSVEP speller were implemented using Matlab/Simulink (Mathworks, USA) and Psychophysics Toolbox extensions [68, 69]. The P300 speller was implemented using BCI2000 [70], which consisted of 36 characters, as did the hybrid speller (Figure 4-3 (b)). The SOA and the flash duration of the P300 speller were determined as an average of those produced by the hybrid speller (SOA of 200 ms and flash duration of 80 ms) because the correlation between the BCI performance and the SOA or the flash duration is still controversial [3, 71, 72]. The stimulator for the spellers was a 24-inch LED monitor (ASUS, VG248QE; resolution: 1920 × 1080) with a refresh rate of 120 Hz.

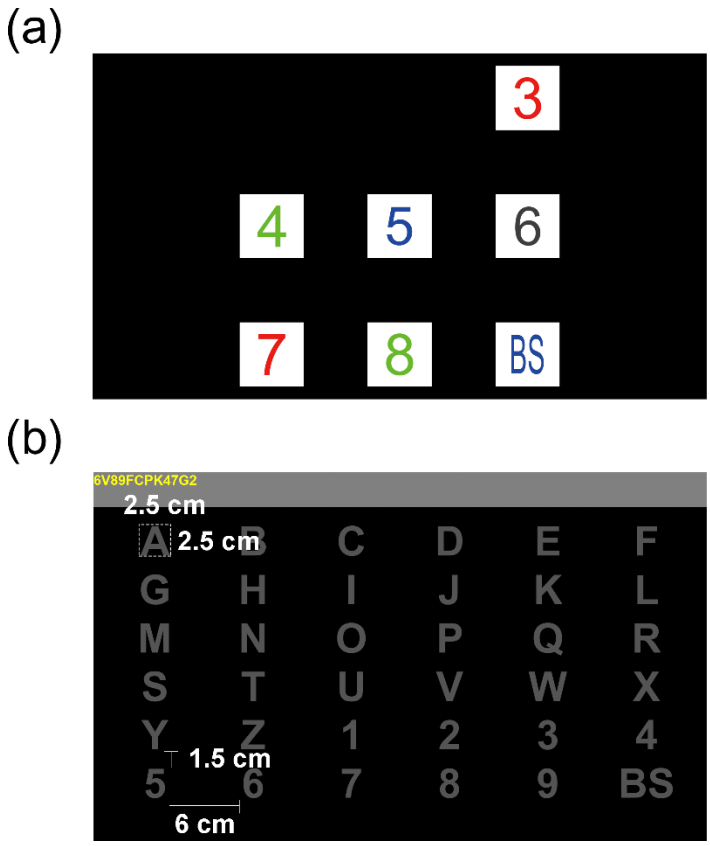

Figure 4-3. Conventional spellers used in this study: (a) SSVEP speller and (b) P300 speller.

4.2.2. Experimental Procedure

All experiments were performed in a general laboratory under common illumination conditions on two or three separate days according to a subject's schedule. However, the experiments with the same speller were conducted on the same day.

For the hybrid or P300 speller, a participant was instructed to focus on a target character and to count the number of times it appeared or flashed. In offline experiments, a trial consisted of ten sequences. Therefore, the P300 stimulus of the hybrid speller appeared ten times during a trial, and the stimulus of the P300 speller flashed twenty times. The subject was exposed to every character in a random order. For the SSVEP speller, the trial stimulation took 9.3 s, which is in accordance with the longest ten-sequence-stimulation time of the hybrid speller (Stimulus 9). A subject focused on one of the seven stimuli during this time, which was repeated 36 times.

In the online experiments, the sequence number was different for each speller: the hybrid and P300 spellers had a trial with sequences equal to the optimal number of sequences; the SSVEP speller flickered for the stimulation time that corresponded to the optimal number of sequences. The optimal number of sequences was determined as the number of sequences with the highest ITR in the offline experiments. The hybrid and P300 speller task was to type the subject's name and his/her phone number once in a run. The task for the SSVEP speller was to type a sequence of numbers consisting of six numbers (3 to 8). Stimulus 9 of the SSVEP speller functioned as "Backspace (BS)" in

the online analysis. The classification result was shown on the screen. The task length remained equal for all the spellers, and the average task length for the subjects was 20.9 characters (range: 18 to 25). Subjects repeated the task twice. All spellers had BS; thus, a subject could correct an error by erasing it and typing a new character. We regarded a run as failed if a subject made more than five consecutive errors for the same target or if the subject was frustrated with repeated errors. Between trials, a period of 5 s was allowed for feedback and a break.

4.2.3. Signal Processing

SSVEP and P300 recognition steps were performed in parallel for the hybrid speller. For SSVEP recognition, the EEG signals were band-pass-filtered at [2 50] Hz and segmented starting from the stimulus onset to the end of the longest stimulation, whose length was $sequence\ number \times 0.93$ s. The SSVEP response was classified using CCA, which showed high accuracy for both single- and dual-frequency SSVEP recognition [5, 43]. The reference signal of CCA for the hybrid speller (Y_{hybrid}) consisted of the sine and cosine of up to the third harmonics of the SSVEP stimulation frequency (f_{SSVEP}) and the P300 stimulation frequency (f_{P300}):

$$Y_{\mathrm{hybrid}_i} = \begin{pmatrix} \sin\left(2\pi f_{\mathrm{SSVEP}_i} t\right) \\ \cos\left(2\pi f_{\mathrm{SSVEP}_i} t\right) \\ \vdots \\ \sin\left(6\pi \mathrm{f}_{\mathrm{SSVEP}_i} t\right) \\ \cos\left(6\pi \mathrm{f}_{\mathrm{SSVEP}_i} t\right) \\ \sin\left(2\pi \mathrm{f}_{\mathrm{P300}_i} t\right) \\ \cos\left(2\pi \mathrm{f}_{\mathrm{P300}_i} t\right) \\ \vdots \\ \sin\left(6\pi \mathrm{f}_{\mathrm{P300}_i} t\right) \\ \cos\left(6\pi \mathrm{f}_{\mathrm{P300}_i} t\right) \end{pmatrix}, \quad i = 1, 2, 3, \ldots, 9. \tag{15}$$

Finally, nine correlations (ρ_{i}) between the transformed SSVEP response and the reference signals were calculated and compared.

In the P300 recognition steps, 800-ms-long EEG segments (480 samples) were extracted starting from the onset of each P300 stimulus for each channel. These segments were then down-sampled to 30 Hz (16 samples) by using a moving average filter. The dimension-reduced segments of all channels were concatenated to yield a single feature vector (x) as [# channels $\times$ 16 samples]. Then, SWLDA was performed to choose 30 statistically significant features and compute the feature weights vector ω [73]. The classifier was trained by a leave-one-out cross validation technique. For the online experiment, the feature weight vector was computed using all the data from the offline experiment. Lastly, the scores of each P300 stimulus were calculated as the sum of the inner product of the feature weight vector and the feature vector.

Taken together, a target on which a subject focused was classified as follows:

$$(l, m) = \underset{i,j}{\arg} \left[\max(\rho_i), \max\left[\sum_{k=1}^{K}(\omega \cdot x_{jk})\right]\right], i \in [1, \dots, 9], j \in [1, \dots, 4] \quad (16)$$

where *i* and *j* denote the numbers of the SSVEP and P300 stimuli of the hybrid speller, respectively; *k* represents the sequence number, and *K* is equal to 10 for the offline analysis and the optimal number of sequences for the online analysis. Consequently, the target was regarded as the m^{th} character (P300 stimulus) of the l^{th} stimulus group (SSVEP stimulus).

For the SSVEP speller, the EEG segments were extracted and analyzed using CCA with a reference signal consisting of up to the third harmonics as (5). The EEG response to a P300 speller was processed with the same P300 recognition steps as those used for the hybrid speller.

4.2.4. Statistical Comparison of the EEG Responses

Segmented SSVEP and P300 responses were statistically compared in the frequency and time domains, respectively ($\alpha = 0.05$). First, the grand average periodograms of the SSVEP were calculated for subjects with respect to the stimulus and the speller. Then, 8th-order SSVEP SNRs were calculated at each stimulation frequency [8, 15] and were statistically compared between spellers as (2). Two-way repeated-measure analysis of variance (RM-ANOVA) was employed to compare SSVEP SNRs with the speller and the stimulation-

frequency factors. Post hoc testing was conducted using a paired *t*-test with Bonferroni correction.

Grand average ERPs over subjects were calculated and plotted using EEGLAB [74]. Pairs of target and non-target ERPs at different electrodes (Fz, Cz, and Pz) and target ERP pairs of different spellers were compared statistically by using a paired *t*-test with Bonferroni correction. Moreover, the P300 amplitude and latency at each electrode were statistically compared between spellers using two-way RM-ANOVA (speller × channel). The P300 amplitude was estimated as the amplitude difference between the peak amplitude within 300 to 600 ms and the pre-stimulus baseline at −200 to 0 ms. P300 latency was estimated as the time from stimulus onset to the peak amplitude between 300 ms and 600 ms [26].

4.2.5. BCI Performance

In addition to accuracy, Wolpaw's ITR is the most common BCI metric that incorporates time [75]. The ITR was calculated using the time taken for feedback and a break as follows:

$$B = \log_2 N + P \log_2 P + (1 - P) \log_2[(1 - P)/(N - 1)] \quad (\text{bits/symbol}), \tag{17}$$

$$T = \begin{cases} \frac{ST \cdot N_S + ITI}{60} & \text{for hybrid and conventional SSVEP spellers} \\ \frac{SOA \cdot N_S \cdot 12 + ITI}{60} & \text{for the conventional P300 speller} \end{cases}, \quad (18)$$

$$ITR = B/T \text{ (bpm)}, \quad (19)$$

where N denotes the number of stimuli (36 for the hybrid and P300 spellers, and 7 for the SSVEP speller) and P represents the accuracy. ST, N_s, and ITI indicate the stimulation time, the sequence number, and the inter-trial interval (5 s), respectively. The equations of T for the hybrid and SSVEP spellers were the same because the SSVEP recognition of the spellers was based on the same stimulation time of a sequence (i.e., 0.933 s).

The BCI performance values were compared with SPSS Statistics 20 (IBM, USA) using two-way RM-ANOVA (speller × sequence number; $\alpha = 0.05$). Significant differences between pairs were found using a paired *t*-test with Bonferroni correction.

4.3. Results

4.3.1. EEG Response to the Hybrid Speller

The EEG response to the hybrid stimuli peaked at the P300 and SSVEP stimulation frequencies (Figure 4-4). Other peaks appeared at the harmonics of the P300 stimulation frequency. Furthermore, compared with the SSVEP stimuli, the hybrid stimuli evoked stronger SSVEPs with significantly higher SSVEP SNR by a factor of 2.24 at the SSVEP stimulation frequency (Figure 4-5; $F = 8.897$, $p = 0.015$). The post hoc analysis revealed that the SNR difference was significant for Stimuli 3 and 4 ($t = 4.752$ and $p < 0.001$ for Stimulus 3; $t = -3.266$ and $p = 0.010$ for Stimulus 4).

The hybrid speller also generated P300 components in the frontal, central, and parietal regions. In Figure 4-6 (a), the grand average ERPs at Fz, Cz, and Pz show apparent positive peaks approximately 450 ms after the P300 stimulus. These positive waves are significantly different from those of the non-target responses ($p < 0.05$). However, the target response at Oz does not show a positive peak and was not significantly different from the non-target response. The P300 latency values showed a significant difference between the spellers ($F = 9.049$, $p = 0.015$; Figure 4-6); the positive peak of the hybrid speller (455 ± 17 ms) occurred 66 ms later than that of the P300 speller (389 ± 15 ms). However, the P300 latency did not differ between channels ($F = 2.259$, $p = 0.133$) and showed no interaction between the speller and channels ($F = 0.440$, $p = 0.651$). P300 amplitudes were not significantly different between the hybrid and P300 spellers (hybrid speller: 3.093 ± 0.279 μV, P300 speller: 2.790 ± 0.405

μV; F = 1.098, p = 0.322) and the channels (F = 2.393, p = 0.120). There was no interaction between the speller and the channel (F = 0.923, p = 0.415).

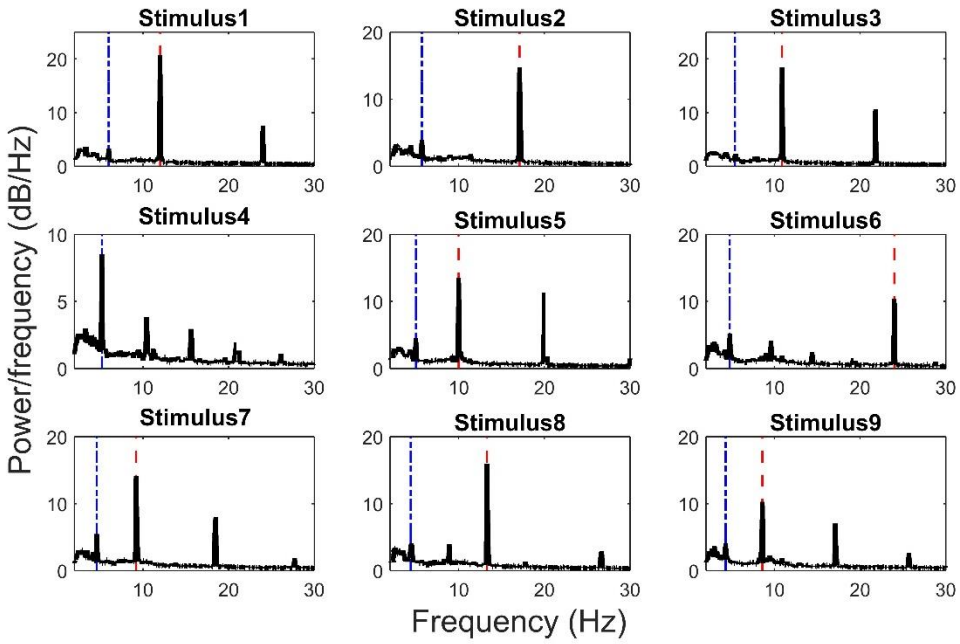

Figure 4-4. Grand average power spectrum of the SSVEP response to each hybrid stimulus at Oz. The dash-dot line represents the P300 stimulation frequency, and the dashed line represents the SSVEP stimulation frequency for each stimulus. The dash-dot and dashed lines of stimulus 4 are overlapped because SSVEP and P300 frequencies are the same.

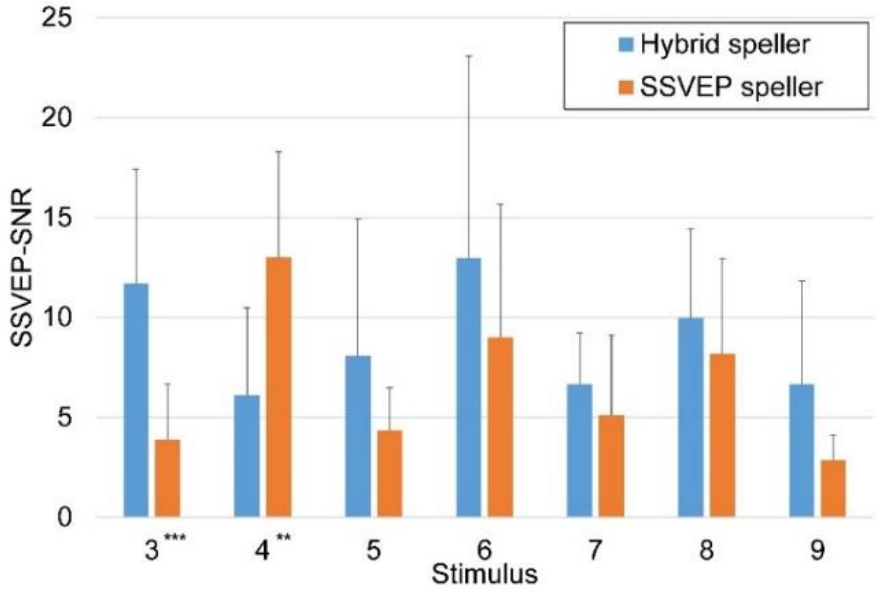

Figure 4-5. Average SSVEP SNR of the hybrid and the SSVEP speller for each stimulus (**: $p < 0.01$, ***: $p < 0.001$).

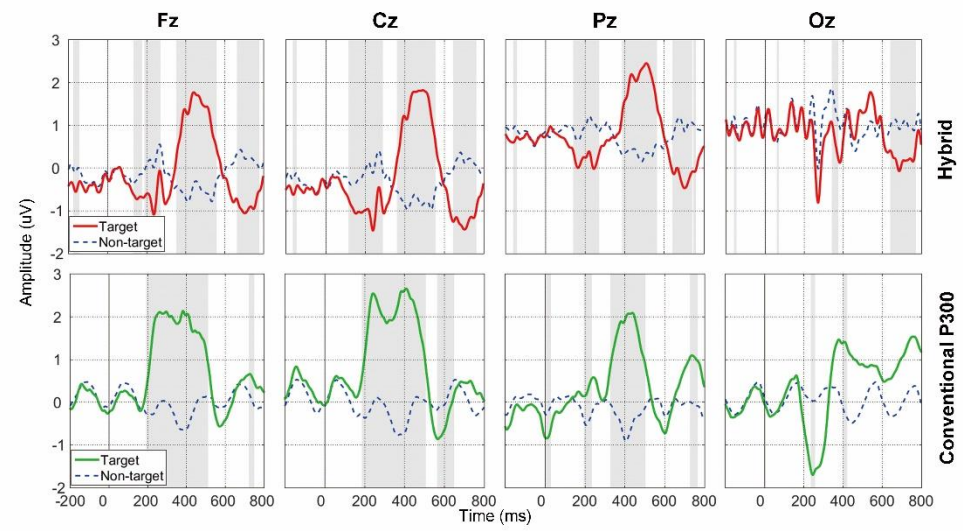

Figure 4-6. Grand average ERP waveforms for different channels. Solid and dashed lines, respectively, represent the target and non-target waveforms of the hybrid speller (top) and the P300 speller (bottom). The gray-shaded regions indicate a significant difference between the two waveforms with $p < 0.05$ (paired *t*-test).

4.3.2. Offline Analysis

An optimized channel set improved the SSVEP recognition rate (Figure 4-7) by 0.017 ± 0.057 for the hybrid speller ($t = 2.977$, $p = 0.004$) and 0.069 ± 0.092 on average for the SSVEP speller ($t = 7.491$, $p < 0.001$). Almost every subject had the highest accuracy with Channel Set 2 for both spellers, which corresponds to the occipital region, which is well known as the place of origin for SSVEP [8]. However, subjects 4, 5, 7, and 10 (S4, S5, S7, and S10, respectively) showed the best performance with Channel Set 3 for the hybrid speller, while S4 and S10 showed the highest accuracy with Channel Set 1 for the SSVEP speller. The channel set that produced the highest accuracy was employed in the online analysis.

The average accuracy over all the sequences of the SSVEP speller (0.855 ± 0.024) was higher than that for the other spellers (hybrid speller: 0.819 ± 0.027, P300 speller: 0.831 ± 0.030; Figure 4-8 (a)), although the difference was not significant ($F = 0.736$, $p = 0.493$). The average ITR was significantly different between spellers ($F = 51.294$, $p < 0.001$) and sequence numbers ($F = 48.211$, $p < 0.001$), and the interaction between the two factors also existed ($F = 22.103$, $p < 0.001$; Figure 4-8 (b)). In particular, the hybrid speller (22.290 ± 1.274 bpm) outperformed the others (11.843 ± 0.743 bpm for the SSVEP speller; 13.251 ± 0.938 bpm for the P300 speller; $p < 0.001$). More importantly, the ITR of the hybrid speller was consistently significantly higher than that of the other spellers for sequence numbers of 3 and above ($p < 0.003$).

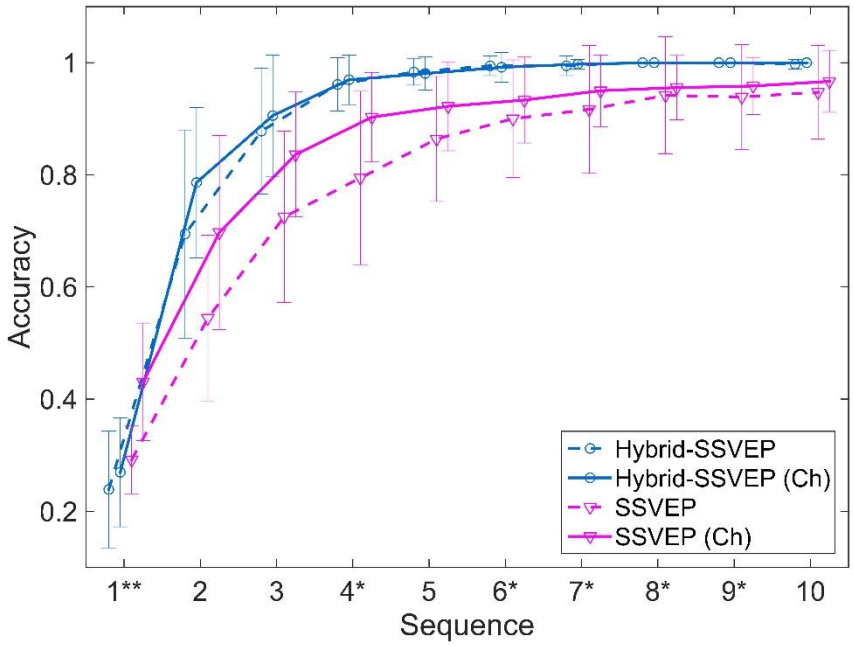

Figure 4-7. SSVEP recognition rate of the SSVEP and hybrid stimuli with or without channel selection in the offline analysis (*: $p < 0.05$; **: $p < 0.01$). The solid lines indicate the SSVEP recognition rate with channel selection.

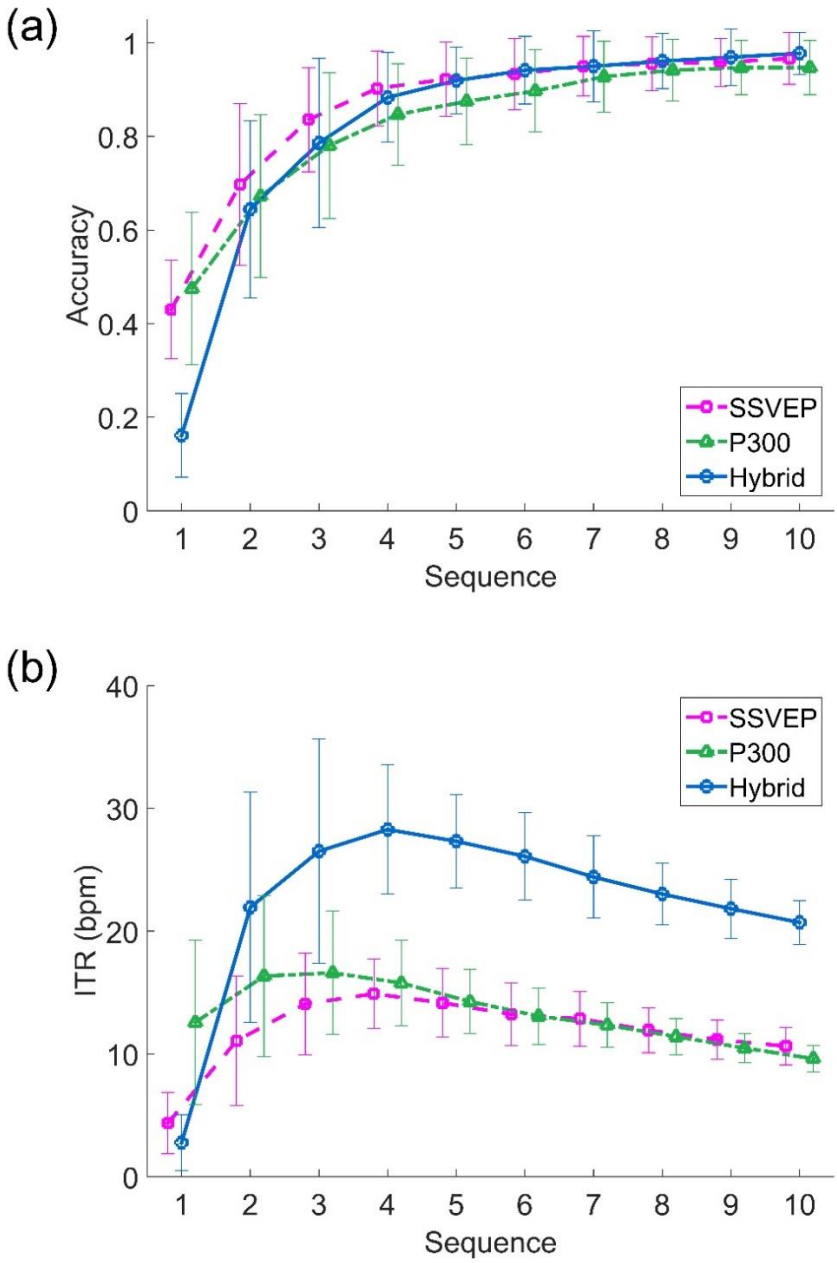

Figure 4-8. BCI performance of the hybrid, SSVEP, and P300 spellers in the offline analysis: (a) Average accuracy and (b) average ITR across subjects

4.3.3. Online Analysis

The optimal number of sequences for each speller differed depending on the subject, as shown in Table 4-2. The average optimal number of sequences was significantly different between the spellers ($F = 6.766$, $p = 0.006$), which seems consistent with ITR trends in the offline analysis (Figure 4-8 (b)).

Table 4-2 shows the accuracy and ITR values for each subject with the different spellers. Each value indicates an average of two runs. S3 could not complete the first run on the hybrid speller; S5 could not complete the second run on the P300 speller or either run on the hybrid speller; and S7 and S10 could not complete either run on the SSVEP speller, yielding very low ITR (Table 4-2). The average accuracy was not significantly different between the spellers ($F = 0.330$, $p = 0.624$). However, the ITR was significantly different between the spellers ($F = 37.159$, $p < 0.001$). In the post hoc test, the hybrid speller showed a significantly higher ITR than the others by more than 11 bpm ($p < 0.002$).

Table 4-2. Results of online experiments in terms of accuracy and ITR with optimal sequence number (SN).

Subject	Hybrid			SSVEP			P300		
	Optimal SN	Accuracy	ITR	Optimal SN	Accuracy	ITR	Optimal SN	Accuracy	ITR
S1	3	.93	34.2	8	.94	11.4	2	.98	30.0
S2	3	.96	36.7	3	.96	19.3	4	.94	18.7
S3	3	.83	28.3	4	1.00	19.3	3	.98	24.2
S4	6	1.00	29.3	9	.96	11.0	3	.96	23.5
S5	3	.70	21.3	6	.94	13.1	2	.62	16.3
S6	4	.98	33.9	7	.95	12.6	4	.88	16.5
S7	3	1.00	39.8	6	.56	3.9	5	.87	14.0
S8	3	.96	36.6	4	.98	18.1	3	.94	22.2
S9	5	.96	29.4	6	.98	14.8	4	.98	20.2
S10	6	.98	28.1	4	.64	6.6	5	.85	13.5
Average	3.9	.93	31.8	5.7	.89	13.0	3.5	.90	19.9

4.4. Discussion

4.4.1. DFSSVEP

In this section, we propose a hybrid BCI speller that flickers at the SSVEP stimulation frequency and presents characters at the P300 stimulation frequency simultaneously. The EEG response to the stimulus shows not only P300 but also the spectral peaks at the sub-harmonic of the SSVEP frequency, which demonstrates that the hybrid speller generates dual-frequency SSVEP. The response to a single-frequency stimulation typically peaks at the fundamental frequency and at the second harmonic. A few rare stimulation frequencies evoke SSVEPs at the second sub-harmonic around the α-band [9]. However, hybrid speller-evoked SSVEPs exhibit peaks at a third, or some other sub-harmonic of the SSVEP stimulation frequency. Considering that the P300 stimulation frequency is a sub-harmonic of the SSVEP stimulation frequency, the peak frequencies can be regarded as a linear combination of the SSVEP and P300 frequencies. The spectral peaks at the linear combination of the stimulation frequencies indicate that the hybrid speller evokes dual-frequency SSVEPs; this is in agreement with the results of previous studies [42, 43]).

It is interesting that the EEG response to the hybrid stimulus is the dual-frequency SSVEP. Usually, a visual stimulus for SSVEP flickers at a constant frequency in a constant shape (e.g., black and white squares or checkerboard). Even a visual stimulus that generates dual-frequency SSVEPs consists of two LEDs flickering at different frequencies without a shape change [39]. However, notwithstanding the fact that the shape (i.e., the character presented on a hybrid

stimulus) changes randomly, a combination of light intensity and shape variations generated dual-frequency SSVEPs successfully.

The dual-frequency stimulation shows some advantages; first, it enhances SSVEPs and improves SSVEP recognition. Second, the use of harmonic frequencies as flickering frequencies increases the number of targets. Third, the simultaneous light intensity and shape variation eliminates unnecessary suspension to generate two types of EEG responses and reduces the stimulation time. All of these effects of dual-frequency stimulation contribute to the improvement of ITR.

4.4.1.1. Improvement in SSVEP Recognition

The dual-frequency stimulation of the hybrid speller enhances the SSVEP SNR and creates features at the harmonics (Figure 4-5), apparently resulting in more accurate SSVEP recognition. Figure 4-7 shows the average SSVEP recognition rate of the hybrid speller and the average accuracy of the SSVEP speller in the offline analysis. The SSVEP recognition rate of the hybrid speller is consistently higher than that of the SSVEP speller except when the sequence number is 1 (Figure 4-7).

The hybrid speller enhanced the SSVEPs in every frequency range including the relatively high frequencies (24 Hz). In the online experiments with the SSVEP speller, two subjects (S7 and S10) failed to complete the whole task, yielding very low ITR. They made almost every error when they tried to type “6” (Stimulus 6). In the offline analysis, their error rate for Stimulus 6

reached 87.5% (7/8). The average SSVEP SNR at the corresponding stimulation frequency (3.250 ± 0.472) was lower than that corresponding to the other stimuli (6.234 ± 4.503). Furthermore, the average SNR for Stimulus 6 of the subjects (3.250 ± 0.472) was lower than that of the other subjects (10.447 ± 6.740). This weak SSVEP would be expected to result in low performance by the SSVEP speller, and the weak response to Stimulus 6 might result from the relatively high SSVEP frequency. Nevertheless, the phenomenon was scarcely observed with the hybrid speller. The two subjects completed the tasks with almost 100% accuracy, and the average SNR of Stimulus 6 (11.140 ± 4.237) was considerably higher than that for the SSVEP speller. We inferred that the dual-frequency stimulation of the hybrid speller enhanced the SSVEPs to Stimulus 6 as well as the other stimuli; therefore, the SSVEP to Stimulus 6 was better recognized with the hybrid speller.

4.4.1.2. Use of Harmonic Frequencies

The hybrid speller augments the number of available targets by successfully employing harmonic frequencies for different stimuli. In an SSVEP-based BCI system, stimulation frequencies should be adjusted according to the refresh rate of the monitor [76], and harmonic frequencies cannot be used for different stimuli. However, the hybrid speller overcame the problem by employing relatively prime P300 stimulation frequencies, which generated harmonics at non-overlapping frequencies, even with harmonic SSVEP frequencies. The hybrid speller succeeded in classifying the two stimuli

by using the non-overlapping harmonic frequencies and achieved a high SSVEP recognition rate.

4.4.1.3. Reduction in Stimulation Time

The hybrid speller reduces the stimulation time compared with a previous hybrid or P300 speller. The combination of intensity and shape variation generates both SSVEP and P300 at the same time; thus, the proposed speller does not require separate stimulation times, as was not the case with a previous hybrid speller [33]. Figure 4-9 illustrates the representative target responses to Stimulus 2 of S10 at Fz, Cz, Pz, and Oz (average of 200 ms before and 800 ms after the appearance of a target character) along with the response spectrum at Oz. Interestingly, a seamless periodic oscillation is observed at Oz, while the P300 component dominates at Fz, Cz, and Pz, as shown in Figure 4-6. The peak frequency of the periodic oscillation at Oz corresponds to the SSVEP stimulation frequency. In addition, the proposed speller reduces the stimulation time compared with the P300 speller by grouping four characters into one stimulus. This strategy results in reducing the number of flashes in a sequence from twelve flashes in the P300 speller (six rows and six columns) to four in the hybrid speller (four P300 stimuli). Simultaneous stimulation and the reduced number of flashes allow the hybrid speller to have a considerably shorter stimulation time (0.93 s) even with a longer stimulus duration and ISI than the P300 speller (stimulation time: 2.4 s).

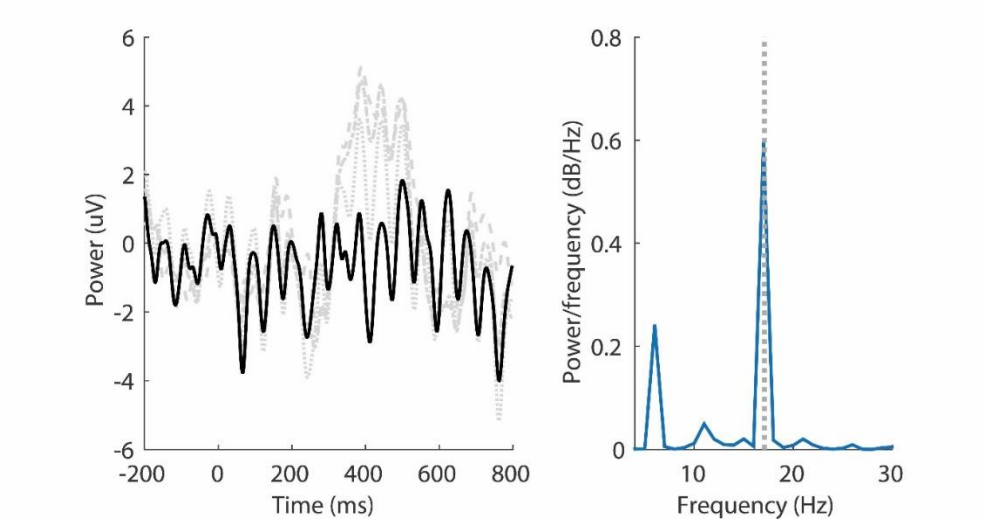

Figure 4-9. Average target response to Stimulus 2 for S10 at Fz (dashed gray line), Cz (dash-dot gray line), Pz (dotted gray line), and Oz (solid black line). The right panel illustrates the power spectrum of the target response at Oz, and the dashed line indicates the corresponding SSVEP stimulation frequency.

4.4.2. ITR Comparison with Conventional Spellers

The characteristics of dual-frequency stimulation in the proposed speller increased the number of targets and reduced the stimulation time; all of these effects contributed to an ITR improvement, shown by Eqs. (17)–(19). In the offline analysis, the ITR of the hybrid speller was considerably larger than that of the other spellers except when the sequence number was 1. In particular, sequence numbers higher than 3 are more likely to be used in practical BCI applications with higher-than-minimum acceptable accuracy (70%) [77, 78]. These results suggest that the hybrid speller is more beneficial in practical use than the conventional spellers. The same conclusion is drawn from the results of the online analysis, in which the hybrid speller showed the best accuracy and ITR. For the hybrid and P300 spellers, the subject-specific parameter (ω) and the channel set in the offline/online tasks and the subject-specific optimal sequence number in the online tasks were employed.

Speller attributes such as the stimulus design and stimulation parameters are different, which makes it difficult to compare the performance of spellers. However, the different attributes reflect and highlight the superiority of the speller proposed in this paper. First, the hybrid speller consists of two more SSVEP stimuli than an SSVEP speller. This difference comes from the ability of the hybrid speller to employ harmonic frequencies for different stimuli, which is an important advantage that results in a positive effect on ITR. Second, the flash duration and the SOA of the P300 stimuli on the hybrid speller vary, and the segmentation performed for the final classification is based on the

longest SOA. In contrast, the stimulation parameters of the P300 speller are set to the median of those of the hybrid speller rather than the longest or the shortest ones. This method avoids any unascertained effects of the stimulation parameters on the BCI performance. However, the hybrid speller showed a higher ITR than did the P300 speller despite the longer stimulation time and the shorter distance between characters in a group. Only P300 latency was different between the spellers (Figure 4-6), and it is presumed to be because of different task complexity; that is, the more densely located characters and the higher degree of noise (white and black squares) in the proposed speller may impede the target recognition and thereby result in a longer P300 latency.

4.4.3. ITR Comparison with Previous Studies

The BCI performance in this study was lower than that observed in previous studies because of the long ITI. A period of 5 s was given to the subjects to rest their eyes and to prepare for the next task. An ITI of 5 s is relatively long considering the stimulation time (9.33 s) and the fact that the ITR is inversely proportional to the time taken, as seen in Eqs. (17)–(19). Therefore, the long interval inevitably results in considerable decreases in the ITR. However, some recent studies take approximately 2 s, and some studies do not even consider the ITI in the ITR calculation. Table 4-3 shows the estimated ITR values from the online analysis for ITIs of 2 s. As the ITI is reduced, the estimated ITR substantially increases by about 20 bpm. The estimated ITR is higher than or equivalent to that of recently proposed hybrid

spellers (Table 4-4). In addition, the estimated practical ITR (PITR) with 2-s ITI (48.2 ± 12.7 bpm) is also equivalent to that of a previous study for increasing ITR (Table 4-4).

However, hybrid BCI with a high ITR has scarcely been investigated to improve the SSVEP recognition rate. Most SSVEP-based hybrid BCIs for improving ITR achieved their goals by increasing the number of stimuli compared with an SSVEP speller and by decreasing the stimulation time compared to a P300 speller. A hybrid SSVEP-P300 speller with a monitor increased ITR by these methods, but failed to improve the SSVEP classification rate. On the contrary, the proposed hybrid speller increased ITR by improving the SSVEP recognition rate as well as by those methods. The SSVEP improvement was obtained by using dual-frequency stimulation with integer-harmonic stimulation frequencies without complex signal processing methods.

Table 4-3. Estimated ITR (bpm) in online analysis with different inter-trial intervals.

	Inter-trial interval	
	5 s	2 s
Average	31.8	49.4
SD	5.9	10.8
Max	39.8	64.6
Min	19.6	31.8

Table 4-4. ITR comparison with recently proposed hybrid SSVEP-P300 spellers

Hybrid SSVEP-P300 speller	# stimuli	ITI (s)	Average ITR (bpm)	SSVEP improvement	Experiment
R. C. Panicker *et al.*, 2011 [79]	36	1	19.05	-	Online
Y. Li *et al.*, 2013 [32]	4	2	22.11	No	Online
L. Bi *et al.*, 2013 [80]	9	-	-	No	Offline
E. Yin *et al.*, 2013 [35]	36	2	56.44	No	Online
M. Xu *et al.*, 2013 [33]	9	0	> 30	-	Offline
M. Xu *et al.*, 2014 [34]	36	1.9	48.5	No	Online
E. Yin *et al.*, 2014 [36]	36	2	48.9 (PITR)	No	Online
B. Z. Allison *et al.*, 2014 [81]	4	0	< 29.8	No	-
M. Wang *et al.*, 2015 [82]	4	-	16.74	No	Offline
Proposed speller [67]	**36**	**2**	**49.4 (PITR: 48.2)**	**Yes**	**Online**

4.4.4. ITR with Different Visual Angle

The accuracy of an SSVEP- or P300 speller is affected by the size of the speller, which is sometimes expressed in degrees of visual angle. SSVEP accuracy decreased as visual angle decreased from 40° to 30° [83]; the reason seems to be that the stimulus size decreased and the distance between stimuli became narrow [44, 84]. Likewise, P300-BCI showed decreasing accuracy when the stimulator was changed from a 17-in monitor to a 5-in mobile phone [85]. Reduced stimulus size and the reduced distance between the stimuli of a smaller stimulator might decrease the P300 accuracy as in the case of the SSVEP accuracy [86].

However, the proposed hybrid speller showed higher P300 accuracy with a smaller visual angle than the P300 speller, contrary to the previous studies (Figure 4-10). This can be attributed to the larger distance between stimuli and larger size of the stimulus of the proposed speller, which overlapped four characters in a stimulus group. Specifically, the visual angle of the proposed speller was 25.8° and for the P300 speller was 41.6° (Figure 4-11). In spite of the smaller size of the speller, the stimulus size and the distance between stimuli of the proposed speller was 2.2 times and 3.6 times greater than those of the P300 speller, respectively. Moreover, the P300 accuracy of the proposed speller was 6 % higher on average than that of the P300 speller (Figure 4-10).

Therefore, the proposed hybrid speller is expected to be more useful in a BCI system with a stimulator of narrow visual angle (e.g., mobile phone or see-through display). With the narrow visual angle, most SSVEP, P300, and hybrid

SSVEP-P300 spellers should decrease the stimulus size and the distance between stimuli because they cannot overlap stimuli. However, the proposed speller generates stimuli overlapped; thus the stimulus size and the distance between stimuli can be larger than those of other spellers. The larger size and distance can make the proposed speller superior to other spellers when it is implemented on a small display or used in a monitor with other applications.

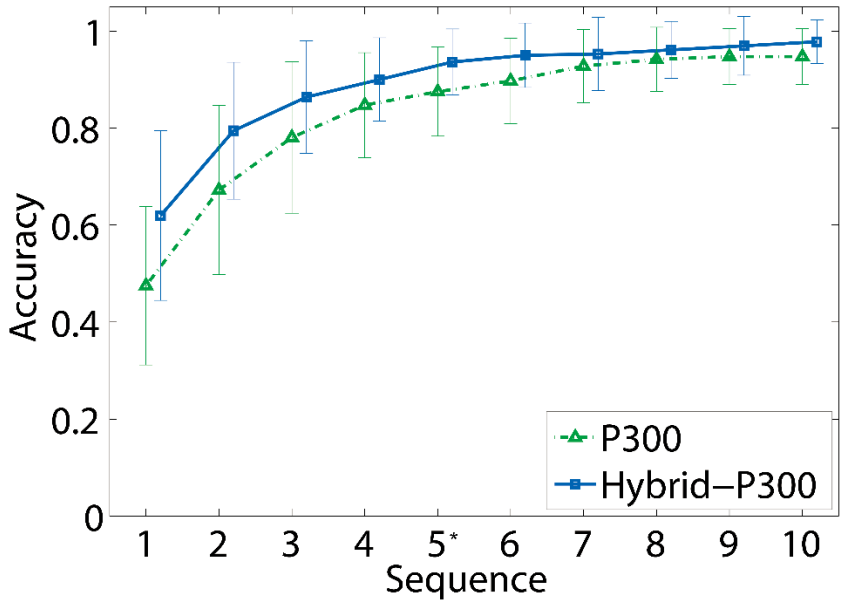

Figure 4-10. P300 accuracy of the P300 and the hybrid spellers in offline analysis (*: $p<0.05$)

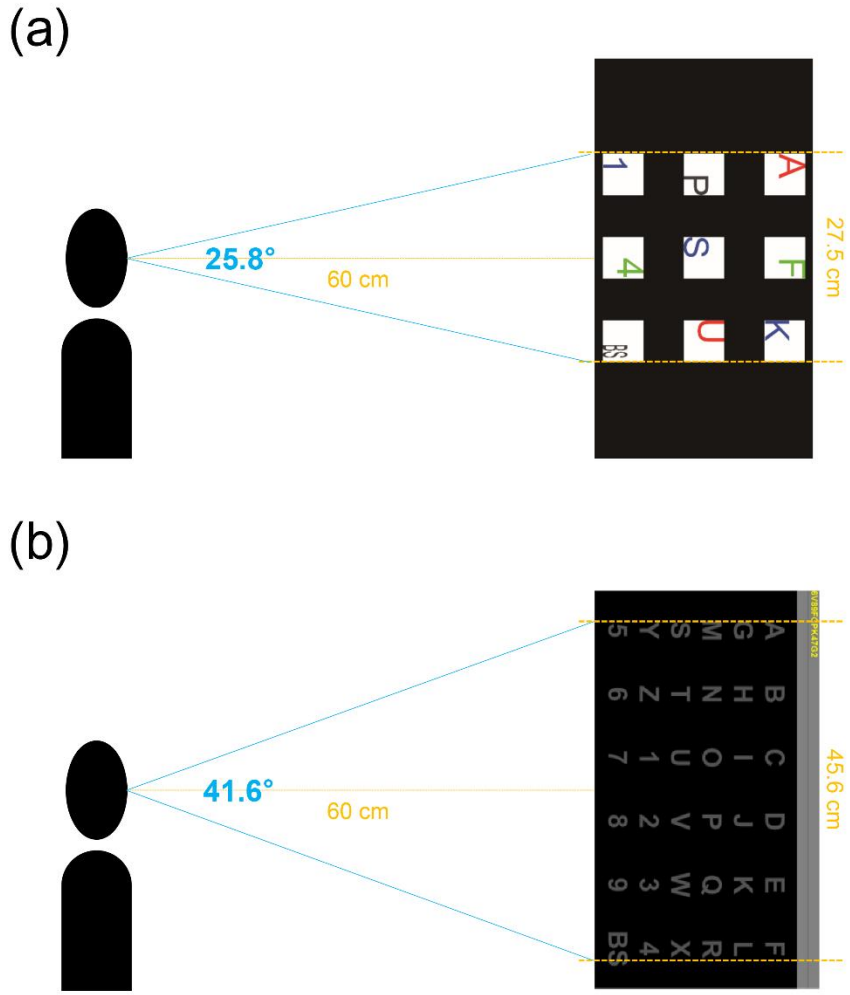

Figure 4-11. Visual angle of (a) the proposed hybrid speller and (b) P300 speller

4.4.5. Limitations

A limitation of the present study is the different stimulation times of the stimuli. When the number of sequences remains constant, a stimulus with a short stimulation time finishes its stimulation earlier than that with a longer stimulation time. We let the stimulus flicker black and white without showing characters after the simulation is completed, but this strategy appears to be time inefficient. Therefore, in the future, we will rearrange the stimulus shapes (i.e., characters) so that all stimuli finish their stimulations at similar times. Another consideration is the visual fatigue caused by the complex stimulation method. The proposed speller presents colorful characters non-uniformly in various directions, which may increase visual fatigue. Thus, modifications in speller design are needed to reduce eye fatigue while maintaining performance.

4.5. Conclusion

The proposed hybrid speller was designed so that a flickering SSVEP stimulus would simultaneously provide a P300 stimulus. The simultaneous stimulation evoked dual-frequency SSVEP, which enhanced SSVEPs and significantly improved the performance of some subjects (S7 and S10). Furthermore, it allowed for harmonic frequencies to be employed as flickering frequencies for different stimuli. These results make up for the weak points of SSVEP-based BCIs with a monitor, such as weak SSVEP and unavailable harmonic frequencies. Further, the hybrid speller reduced the number of flashes from twelve (RC paradigm) to four (the hybrid speller), thereby reducing the stimulation time and improving ITR compared to a P300 speller. In the online analysis, the ITR of the hybrid speller was considerably greater than that of the conventional SSVEP and P300 spellers with accuracy of more than 90%.

5

Conclusion

SSVEP-based BCIs have been widely investigated because of not only their simple system but also high accuracy and speed. In particular, considerably high ITR and low inter- and intra- subject variability raise hopes that it can improve the quality of life of the severely disabled. However, a flickering stimulus causes high eye fatigue so that it makes long-term use difficult. Furthermore, limitation in selection of a stimulation frequency and low SSVEP power with a monitor prevents realization of a simple device, and consequentially, practical use.

In this thesis, dual-frequency SSVEP-based BCIs have been investigated to resolve these issues. First, spectral characteristics of dual-frequency SSVEPs have been identified. From the result, a frequency recognition method that considers harmonics was developed and examined. Then, two dual-frequency SSVEP-based BCIs were designed, each of which addresses the issues

respectively: AM-SSVEP based BCI and hybrid BCI speller. AM-SSVEP based BCI significantly reduced eye fatigue by combining high carrier frequency and low modulating frequency. Furthermore, its BCI performance was maintained high with an accuracy of 91.2% and ITR of 30.4 bpm in online experiments. The hybrid BCI speller produced 36 stimuli with only nine flickering frequencies, and harmonic frequencies were successfully employed in a BCI speller. Moreover, SSVEPs evoked by the hybrid stimuli were stronger with a higher SSVEP recognition rate than those by single-frequency flickering stimuli. These novel BCI systems improved an SSVEP-based BCI system with equivalent or higher performance compared with conventional systems.

The proposed systems can be improved by combining recently reported techniques. First, AM-SSVEP based BCI uses LEDs as a stimulator to generate a modulated signal, which makes the system complex. However, a recent report demonstrated that a monitor can generate sine stimulation in both low- and high-frequency ranges [25]. Thus, AM-SSVEP based BCI can be tested with a monitor to simplify the system. Second, the proposed hybrid speller can reduce eye fatigue resulting from colorful stimuli. It can be obtained by changing the color arrangement or location of stimuli, however, while being careful not to degrade the P300 classification performance. On the other hand, machine learning techniques such as dynamic stopping can be used to increase classification speed.

The dual-frequency SSVEP-based BCIs have been developed to complement weaknesses and to be used in real life. To do that, the developed

systems should be examined by potential users. SSVEP-based BCIs have had less testing by the disabled than P300- or SMR-based BCIs. Through a long-term test by the severely disabled, SSVEP-based BCIs should be complemented and finally contribute to improving a patient's life.

6

References

[1] M. A. Lebedev and M. A. L. Nicolelis, "Brain–machine interfaces: past, present and future," *Trends Neurosci.*, vol. 29, no. 9, pp. 536-546, 2006.

[2] V. Morash, O. Bai, S. Furlani, P. Lin, and M. Hallett, "Classifying EEG signals preceding right hand, left hand, tongue, and right foot movements and motor imageries," *Clin. Neurophysiol.*, vol. 119, no. 11, pp. 2570-2578, 2008.

[3] L. A. Farwell and E. Donchin, "Talking off the top of your head: toward a mental prosthesis utilizing event-related brain potentials," *Electroencephalogr. Clin. Neurophysiol.*, vol. 70, no. 6, pp. 510-523, 1988.

[4] E. Lew, R. Chavarriaga, S. Silvoni, and J. d. R. Millán, "Detection of self-paced reaching movement intention from EEG signals," *Front. Neuroeng.*, vol. 5, p. 13, 2012.

[5] G. Bin, X. Gao, Z. Yan, B. Hong, and S. Gao, "An online multi-channel SSVEP-based brain-computer interface using a canonical correlation analysis method," *J. Neural Eng.*, vol. 6, no. 4, p. 046002, 2009.

[6] A. Z. Snyder, "Steady-state vibration evoked potentials: description of

technique and characterization of responses," *Electroencephalogr. Clin. Neurophysiol.*, vol. 84, no. 3, pp. 257-268, 1992.

[7] G. Pfurtscheller, B. Z. Allison, C. Brunner, G. Bauernfeind, T. Solis-Escalante, R. Scherer, *et al.*, "The hybrid BCI," *Front. Neurosci.*, vol. 4, p. 30, 2010.

[8] F.-B. Vialatte, M. Maurice, J. Dauwels, and A. Cichocki, "Steady-state visually evoked potentials: Focus on essential paradigms and future perspectives," *Prog. Neurobiol.*, vol. 90, no. 4, pp. 418-438, 2010.

[9] C. S. Herrmann, "Human EEG responses to 1–100 Hz flicker: resonance phenomena in visual cortex and their potential correlation to cognitive phenomena," *Exp. Brain Res.*, vol. 137, no. 3-4, pp. 346-353, 2001.

[10] B. Graimann, B. Allison, and G. Pfurtscheller, *Brain-computer interfaces : revolutionizing human-computer interaction*. New York: Springer-Verlag, 2010.

[11] E. Pasqualotto, S. Federici, and M. O. Belardinelli, "Toward functioning and usable brain-computer interfaces (BCIs): a literature review," *Disabil. Rehabil. Assist. Technol.*, vol. 7, no. 2, pp. 89-103, 2012.

[12] H. Cecotti, "A self-paced and calibration-less SSVEP-based brain-computer interface speller," *IEEE Trans. Neural Syst. Rehabil. Eng.*, vol. 18, no. 2, pp. 127-133, 2010.

[13] K. Shyu, Y. J. Chiu, P. L. Lee, M. H. Lee, J. J. Sie, C. H. Wu, *et al.*, "Total Design of an FPGA-Based Brain Computer Interface Control Hospital Bed Nursing System," *IEEE Trans. Ind. Electron.*, vol. 60, no. 7, pp. 2731-2739, 2013.

[14] R. Ortner, B. Z. Allison, G. Korisek, H. Gaggl, and G. Pfurtscheller, "An SSVEP BCI to Control a Hand Orthosis for Persons With Tetraplegia," *IEEE Trans. Neural Syst. Rehabil. Eng.*, vol. 19, no. 1, pp. 1-5, 2011.

[15] Y. Wang, R. P. Wang, X. R. Gao, B. Hong, and S. K. Gao, "A practical VEP-based brain-computer interface," *IEEE Trans. Neural Syst. Rehabil. Eng.*, vol. 14, no. 2, pp. 234-239, 2006.

[16] J. J. Wilson and R. Palaniappan, "Analogue mouse pointer control via an online steady state visual evoked potential (SSVEP) brain-computer interface," *J. Neural Eng.*, vol. 8, no. 2, pp. 1-6, 2011.

[17] Y. T. Wang, Y. Wang, and T. P. Jung, "A cell-phone-based brain-computer interface for communication in daily life," *J. Neural Eng.*, vol. 8, no. 2, pp. 1-5, 2011.

[18] L. Fang-Cheng, J. K. Zao, T. Kuan-Chung, W. Yijun, H. Yi-Pai, C. Che-Wei, *et al.*, "SNR analysis of high-frequency steady-state visual evoked potentials from the foveal and extrafoveal regions of Human Retina," in *Conf. Proc. IEEE Eng. Med. Biol. Soc.*, San Diego, USA, 2012, pp. 1810-1814.

[19] A. Wilkins, J. Veitch, and B. Lehman, "LED lighting flicker and potential health concerns: IEEE standard PAR1789 update," in *Proc. IEEE Energy Convers. Congr. Expo.*, 2010, pp. 171-178.

[20] S. Muller, P. F. Diez, T. F. Bastos-Filho, M. Sarcinelli-Filho, V. Mut, and E. Laciar, "SSVEP-BCI implementation for 37–40 Hz frequency range," in *Conf. Proc. IEEE Eng. Med. Biol. Soc.*, Boston, USA, 2011, pp. 6352-6355.

[21] G. G. Molina and V. Mihajlovic, "Spatial filters to detect steady-state visual evoked potentials elicited by high frequency stimulation: BCI application," *Biomed. Tech. (Berl.)*, vol. 55, no. 3, pp. 173-182, 2010.

[22] I. Volosyak, D. Valbuena, T. Luth, T. Malechka, and A. Graser, "BCI Demographics II: How Many (and What Kinds of) People Can Use a High-Frequency SSVEP BCI?," *IEEE Trans. Neural Syst. Rehabil. Eng.*, vol. 19, no. 3, pp. 232-239, 2011.

[23] Z. Wu, Y. Lai, Y. Xia, D. Wu, and D. Yao, "Stimulator selection in SSVEP-based BCI," *Med. Eng. Phys.*, vol. 30, no. 8, pp. 1079-1088,

2008.

[24] E. Yin, Z. Zhou, J. Jiang, Y. Yu, and D. Hu, "A Dynamically Optimized SSVEP Brain-Computer Interface (BCI) Speller," *IEEE Trans. Biomed. Eng.*, vol. 62, no. 6, pp. 1447-1456, 2015.

[25] X. Chen, Z. Chen, S. Gao, and X. Gao, "A high-ITR SSVEP-based BCI speller," *Brain-Comp. Interfaces*, vol. 1, no. 3-4, pp. 181-191, 2014.

[26] J. Polich, "Neuropsychology of P300," in *Oxford handbook of event-related potential components*, E. S. Kappenman and S. J. Luck, Eds., ed New York: Oxford University Press, 2012, pp. 159-188.

[27] J. T. Cacioppo, L. G. Tassinary, and G. Berntson, *Handbook of psychophysiology*: Cambridge University Press, 2007.

[28] S. M. Kamp, A. R. Murphy, and E. Donchin, "The Component Structure of Event-Related Potentials in the P300 Speller Paradigm," *IEEE Trans. Neural Syst. Rehabil. Eng.*, vol. 21, no. 6, pp. 897-907, 2013.

[29] A. Furdea, S. Halder, D. J. Krusienski, D. Bross, F. Nijboer, N. Birbaumer, *et al.*, "An auditory oddball (P300) spelling system for brain-computer interfaces," *Psychophysiol.*, vol. 46, no. 3, pp. 617-625, 2009.

[30] J. Hohne, K. Krenzlin, S. Dahne, and M. Tangermann, "Natural stimuli improve auditory BCIs with respect to ergonomics and performance," *J. Neural Eng.*, vol. 9, no. 4, p. 045003, 2012.

[31] R. Corralejo, L. Nicolás-Alonso, D. Á lvarez, and R. Hornero, "A P300-based brain–computer interface aimed at operating electronic devices at home for severely disabled people," *Med. Biol. Eng. Comput.*, vol. 52, no. 10, pp. 861-872, 2014.

[32] Y. Li, J. Pan, F. Wang, and Z. Yu, "A hybrid BCI system combining P300 and SSVEP and iIts application to wheelchair control," *IEEE Trans. Biomed. Eng.*, vol. 60, no. 11, pp. 3156-3166, 2013.

[33] M. Xu, H. Qi, B. Wan, T. Yin, Z. Liu, and D. Ming, "A hybrid BCI

speller paradigm combining P300 potential and the SSVEP blocking feature," *J. Neural Eng.*, vol. 10, no. 2, p. 026001, 2013.

[34] M. Xu, L. Chen, L. Zhang, H. Qi, L. Ma, J. Tang, *et al.*, "A visual parallel-BCI speller based on the time-frequency coding strategy," *J. Neural Eng.*, vol. 11, no. 2, p. 026014, 2014.

[35] E. Yin, Z. Zhou, J. Jiang, F. Chen, Y. Liu, and D. Hu, "A novel hybrid BCI speller based on the incorporation of SSVEP into the P300 paradigm," *J. Neural Eng.*, vol. 10, no. 2, p. 026012, 2013.

[36] E. Yin, Z. Zhou, J. Jiang, F. Chen, Y. Liu, and D. Hu, "A speedy hybrid BCI spelling approach combining P300 and SSVEP," *IEEE Trans. Biomed. Eng.*, vol. 61, no. 2, pp. 473-483, 2014.

[37] Y. Zheng, G. Xiaorong, B. Guangyu, H. Bo, and G. Shangkai, "A half-field stimulation pattern for SSVEP-based brain-computer interface," in *Conf. Proc. IEEE Eng. Med. Biol. Soc.*, Minneapolis, 2009, pp. 6461-6464.

[38] P. L. Lee, C. L. Yeh, J. Y. S. Cheng, C. Y. Yang, and G. Y. Lan, "An SSVEP-Based BCI Using High Duty-Cycle Visual Flicker," *IEEE Trans. Biomed. Eng.*, vol. 58, no. 12, pp. 3350-3359, 2011.

[39] K. K. Shyu, P. L. Lee, Y. J. Liu, and J. J. Sie, "Dual-frequency steady-state visual evoked potential for brain computer interface," *Neurosci. Lett.*, vol. 483, no. 1, pp. 28-31, 2010.

[40] H.-J. Hwang, D. H. Kim, C.-H. Han, and C.-H. Im, "A new dual-frequency stimulation method to increase the number of visual stimuli for multi-class SSVEP-based brain–computer interface (BCI)," *Brain Res.*, vol. 1515, pp. 66-77, 2013.

[41] M. H. Chang, H. S. Kim, J. S. Lee, and K. S. Park, "Dual-frequency steady-state visual evoked potentials to different shapes of stimuli," in *Proc. 47th Conf. Korea Soc. Med. Biol. Eng.*, 2013.

[42] T. M. Srihari Mukesh, V. Jaganathan, and M. R. Reddy, "A novel multiple frequency stimulation method for steady state VEP based

brain computer interfaces," *Physiol. Meas.,* vol. 27, no. 1, pp. 61-71, 2006.

[43] M. H. Chang and K. S. Park, "Frequency recognition methods for dual-frequency SSVEP based brain-computer interface," in *Conf. Proc. IEEE Eng. Med. Biol. Soc.*, Osaka, Japan, 2013, pp. 2220-2223.

[44] J. Bieger and G. G. Molina, "Light Stimulation Properties to Influence Brain Activity," Eindhoven, the Netherlands TN-2010-00315, Sep 2010.

[45] F. Teng, A. M. Choong, S. Gustafson, D. Waddell, P. Lawhead, and Y. Chen, "Steady state visual evoked potentials by dual sine waves," in *Proc. Ann. ACM SE Reg. Conf.,* 2010, pp. 50-53.

[46] M. Lopez-Gordo, A. Prieto, F. Pelayo, and C. Morillas, "Use of phase in brain–computer interfaces based on steady-state visual evoked potentials," *Neural Process. Lett.,* vol. 32, no. 1, pp. 1-9, 2010.

[47] M. H. Chang, H. J. Baek, S. M. Lee, and K. S. Park, "An amplitude-modulated visual stimulation for reducing eye fatigue in SSVEP-based brain–computer interfaces," *Clin. Neurophysiol.,* vol. 125, no. 7, pp. 1380-1391, 2014.

[48] M. Cheng, X. Gao, S. Gao, and D. Xu, "Design and implementation of a brain-computer interface with high transfer rates," *IEEE Trans. Biomed. Eng.,* vol. 49, no. 10, pp. 1181-1186, 2002.

[49] S. P. Kelly, E. C. Lalor, R. B. Reilly, and J. J. Foxe, "Visual spatial attention tracking using high-density SSVEP data for independent brain-computer communication," *IEEE Trans. Neural Syst. Rehabil. Eng.*, vol. 13, no. 2, pp. 172-178, 2005.

[50] F. Lotte, M. Congedo, A. Lecuyer, F. Lamarche, and B. Arnaldi, "A review of classification algorithms for EEG-based brain-computer interfaces," *J. Neural Eng.,* vol. 4, no. 2, pp. R1-R13, 2007.

[51] G. Hakvoort, B. Reuderink, and M. Obbink, "Comparison of PSDA and CCA detection methods in a SSVEP-based BCI-system," Centre

for Telematics and Information Technology University of Twente TR-CTIT-11-03, Feb 2011.

[52] L. Frenzel, *Principles of electronic communication systems*. New York: McGraw-Hill, Inc., 2007.

[53] M. Fatourechi, A. Bashashati, R. K. Ward, and G. E. Birch, "EMG and EOG artifacts in brain computer interface systems: A survey," *Clin. Neurophysiol.*, vol. 118, no. 3, pp. 480-494, 2007.

[54] P. F. Diez, V. A. Mut, E. M. Avila Perona, and E. Laciar Leber, "Asynchronous BCI control using high-frequency SSVEP," *J. Neuroeng. Rehabil.*, vol. 8, no. p. 39, 2011.

[55] A. Luo and T. J. Sullivan, "A user-friendly SSVEP-based brain-computer interface using a time-domain classifier," *J. Neural Eng.*, vol. 7, no. 2, pp. 1-10, 2010.

[56] L. Eui Chul, H. Hwan, and P. Kang Ryoung, "The comparative measurements of eyestrain caused by 2D and 3D displays," *IEEE Trans. Consum. Electr.*, vol. 56, no. 3, pp. 1677-1683, 2010.

[57] C. Kim, S. Park, M. Won, M. Whang, and E. Lee, "Autonomic Nervous System Responses Can Reveal Visual Fatigue Induced by 3D Displays," *Sensors*, vol. 13, no. 10, p. 13054, 2013.

[58] Y. Punsawad and Y. Wongsawat, "User performance evaluation with visual stimulator regulation of SSVEP-based BCI system," in *Asia-Pacific Signal and Information Processing Association, 2014 Annual Summit and Conference (APSIPA)*, 2014, pp. 1-4.

[59] J. R. Wolpaw, N. Birbaumer, W. J. Heetderks, D. J. McFarland, P. H. Peckham, G. Schalk, *et al.*, "Brain-computer interface technology: a review of the first international meeting," *IEEE Trans. Biomed. Eng.*, vol. 8, no. 2, pp. 164-173, 2000.

[60] P. L. Lee, J. J. Sie, Y. J. Liu, C. H. Wu, M. H. Lee, C. H. Shu, *et al.*, "An SSVEP-actuated brain computer interface using phase-tagged flickering sequences: a cursor system," *Ann. Biomed. Eng.*, vol. 38, no.

7, pp. 2383-2397, 2010.

[61] B. Allison, T. Luth, D. Valbuena, A. Teymourian, I. Volosyak, and A. Graser, "BCI Demographics: How Many (and What Kinds of) People Can Use an SSVEP BCI?," *IEEE Trans. Neural Syst. Rehabil. Eng.*, vol. 18, no. 2, pp. 107-116, 2010.

[62] H. Cecotti, "Spelling with non-invasive Brain-Computer Interfaces--current and future trends," *J. Physiol. -Paris*, vol. 105, no. 1-3, pp. 106-114, 2011.

[63] A. Bashashati, M. Fatourechi, R. K. Ward, and G. E. Birch, "A survey of signal processing algorithms in brain–computer interfaces based on electrical brain signals," *J. Neural Eng.*, vol. 4, no. 2, pp. R32-R57, 2007.

[64] C.-K. Kim, S. Lee, D. Koh, and B.-M. Kim, "Development of wireless NIRS system with dynamic removal of motion artifacts," *Biomed. Eng. Lett.*, vol. 1, no. 4, pp. 254-259, 2011.

[65] H. J. Baek, H. J. Lee, Y. G. Lim, and K. S. Park, "Conductive Polymer Foam Surface Improves the Performance of a Capacitive EEG Electrode," *IEEE Trans. Biomed. Eng.*, vol. 59, no. 12, pp. 3422-3431, 2012.

[66] C. Grozea, C. D. Voinescu, and S. Fazli, "Bristle-sensor—slow-cost flexible passive dry EEG electrodes for neurofeedback and BCI applications," *J. Neural Eng.*, vol. 8, no. 2, pp. 1-8, 2011.

[67] M. H. Chang, J. S. Lee, J. Heo, and K. S. Park, "Eliciting dual-frequency SSVEP using a hybrid SSVEP-P300 BCI," *J. Neurosci. Meth.*, vol. 258, pp. 104-113, 2016.

[68] D. G. Pelli, "The VideoToolbox software for visual psychophysics: transforming numbers into movies," *Spat. Vis.*, vol. 10, no. 4, pp. 437-442, 1997.

[69] D. H. Brainard, "The Psychophysics Toolbox," *Spat. Vis.*, vol. 10, no. 4, pp. 433-436, 1997.

[70] G. Schalk, D. J. McFarland, T. Hinterberger, N. Birbaumer, and J. R. Wolpaw, "BCI2000: a general-purpose brain-computer interface (BCI) system," *IEEE Trans. Biomed. Eng.*, vol. 51, no. 6, pp. 1034-1043, 2004.

[71] Y. Li, S. Bahn, C. S. Nam, and J. Lee, "Effects of Luminosity Contrast and Stimulus Duration on User Performance and Preference in a P300-Based Brain–Computer Interface," *Int. J. Hum.-Comput. Int.*, vol. 30, no. 2, pp. 151-163, 2013.

[72] E. W. Sellers, D. J. Krusienski, D. J. McFarland, T. M. Vaughan, and J. R. Wolpaw, "A P300 event-related potential brain–computer interface (BCI): The effects of matrix size and inter stimulus interval on performance," *Biol. Psychol.*, vol. 73, no. 3, pp. 242-252, 2006.

[73] D. J. Krusienski, E. W. Sellers, D. J. McFarland, T. M. Vaughan, and J. R. Wolpaw, "Toward enhanced P300 speller performance," *J. Neurosci. Meth.*, vol. 167, no. 1, pp. 15-21, 2008.

[74] A. Delorme and S. Makeig, "EEGLAB: an open source toolbox for analysis of single-trial EEG dynamics including independent component analysis," *J. Neurosci. Meth.*, vol. 134, no. 1, pp. 9-21, 2004.

[75] P. Yuan, X. Gao, B. Allison, Y. Wang, G. Bin, and S. Gao, "A study of the existing problems of estimating the information transfer rate in online brain–computer interfaces," *J. Neural Eng.*, vol. 10, no. 2, p. 026014, 2013.

[76] I. Volosyak, H. Cecotti, and A. Graser, "Optimal visual stimuli on LCD screens for SSVEP based Brain-Computer Interfaces," in *Proc. IEEE/EMBS 4th Int. Conf. Neural Eng. (NER'09)*, 2009, pp. 447-450.

[77] S. C. Kleih, F. Nijboer, S. Halder, and A. Kübler, "Motivation modulates the P300 amplitude during brain–computer interface use," *Clin. Neurophysiol.*, vol. 121, no. 7, pp. 1023-1031, 2010.

[78] A. Kübler, B. Kotchoubey, J. Kaiser, J. R. Wolpaw, and N. Birbaumer, "Brain–computer communication: Unlocking the locked in," *Psychol.*

Bull., vol. 127, no. 3, pp. 358-375, 2001.

[79] R. C. Panicker, S. Puthusserypady, and S. Ying, "An Asynchronous P300 BCI With SSVEP-Based Control State Detection," *IEEE Trans. Biomed. Eng.*, vol. 58, no. 6, pp. 1781-1788, 2011.

[80] B. Luzheng, J. Ke, F. Xin-an, and L. Yun, "A SSVEP brain-computer interface with the hybrid stimuli of SSVEP and P300," in *Complex Medical Engineering (CME), 2013 ICME International Conference on*, 2013, pp. 211-214.

[81] B. Z. Allison, J. Jin, Y. Zhang, and X. Wang, "A four-choice hybrid P300/SSVEP BCI for improved accuracy," *Brain-Comp. Interfaces*, vol. 1, no. 1, pp. 17-26, 2014.

[82] M. Wang, I. Daly, B. Z. Allison, J. Jin, Y. Zhang, L. Chen, *et al.*, "A new hybrid BCI paradigm based on P300 and SSVEP," *J. Neurosci. Methods*, vol. 244, pp. 16-25, 2015.

[83] H. J. Hwang, J. H. Lim, Y. J. Jung, H. Choi, S. W. Lee, and C. H. Im, "Development of an SSVEP-based BCI spelling system adopting a QWERTY-style LED keyboard," *J. Neurosci. Methods*, vol. 208, no. 1, pp. 59-65, 2012.

[84] K. B. Ng, A. P. Bradley, and R. Cunnington, "Stimulus specificity of a steady-state visual-evoked potential-based brain-computer interface," *J. Neural Eng.*, vol. 9, no. 3, p. 036008, 2012.

[85] Y. Li, C. S. Nam, B. B. Shadden, and S. L. Johnson, "A P300-Based Brain–Computer Interface: Effects of Interface Type and Screen Size," *Int. J. Hum.-Comput. Int.*, vol. 27, no. 1, pp. 52-68, 2010.

[86] M. Salvaris and F. Sepulveda, "Visual modifications on the P300 speller BCI paradigm," *J. Neural Eng.*, vol. 6, no. 4, p. 046011, 2009.

국문 초록

낮은 시각 피로도와 높은 정확도를 위한 이중주파수 SSVEP 기반 BCI

안정상태 시각유발전위는 다른 뇌파에 비해 신호대잡음비가 높고 트레이닝이 거의 필요 없어 뇌-컴퓨터 인터페이스에 많이 이용된다. 이로 인해 안정상태 시각유발전위 기반 뇌-컴퓨터 인터페이스는 복잡한 신호 처리 기술이 없이도 높은 정확도를 보이며, 높은 정보 전달률을 가지는 뇌-컴퓨터 인터페이스 시스템이 개발되었다. 그러나 안정상태 시각유발전위는 높은 시각 피로도를 유발하고 간질성 발작을 일으킬 확률이 높다. 또한, 배수 성분의 주파수를 사용하지 못 하는 등 자극 주파수 선택에 제한이 있고, 모니터를 자극기로 사용할 경우 안정상태 시각유발전위의 크기가 감소하는 문제점이 있다. 본 연구에서는 이중 주파수 안정상태 시각유발전위를 이용하여 위의 문제점들을 해결하고자 하였다.

먼저 이중 주파수 안정상태 시각유발전위의 주파수 특성을 살펴보고 분류 알고리즘을 제안하였다. 각각의 방법은 파워 스펙트럼 밀도 분석과 정준상관분석에 기반한 방법으로, 기존의 단일 주파수 안정상태 시각유발전위 분류를 위한 방법을 이중 주파수 안정상태 시각유발전위의 주파수 특성에 맞추어 개선하였다. 분석 결과 새로운 형태의 기준 신호를 이용한 정준상관분석법이 가장 높은 정확도를 보였으며, 특히 자극 주파수 성분과 하모닉 성분을 함께 고려할 경우 정확도가 더 높게 나타났다.

다음으로는 진폭 변조된 시각자극에 의해 발생하는 안정상태 시각유발전위를 이용해 시각 피로도를 낮추고자 하였다. 진폭

변조된 시각 자극은 40 Hz 이상의 높은 캐리어 주파수와 알파 밴드 영역(9-12 Hz)의 낮은 모듈레이팅 주파수의 두 사인 함수의 곱으로 발생되었다. 높은 캐리어 주파수는 시각 피로도를 줄이기 위해, 낮은 모듈레이팅 주파수는 저주파수 하모닉 성분을 이용하기 위해 적용되었다. 피험자 각각 최적화된 주파수 조합을 구하여 온라인 실험에 적용한 결과 제안한 시스템의 성능은 기존의 고주파수 또는 저주파수 안정상태 시각유발전위 기반 뇌-컴퓨터 인터페이스와 동등하게 나타났다. 또한, 온라인 실험에서 피험자의 주관적 평가를 통해 시각 피로도가 유의미하게 낮아졌음을 확인하였다.

세 번째로는 주파수 제한 문제를 극복하고 정확도를 향상시키기 위해 안정상태 시각유발전위와 P300 전위를 조합한 하이브리드 뇌-컴퓨터 인터페이스 스펠러를 제안하였다. 하이브리드 스펠러는 서로 다른 주파수로 깜빡이는 아홉 개의 자극 군으로 구성되었으며, 각 자극 군은 서로 다른 네 개의 알파벳을 임의의 순서로 보여주었다. 이를 통해 깜빡이는 자극 군과 주기적으로 변하는 글자들은 이중 주파수 안정상태 시각유발전위를 일으켰으며, 글자로 이루어진 오드볼 자극은 P300 전위를 유발하였다. 오프라인/온라인 실험을 통해 제안된 하이브리드 스펠러와 기존의 안정상태 시각유발전위 또는 P300 기반 스펠러들의 성능을 비교하였다. 분석 결과 제안한 하이브리드 스펠러가 이중 주파수 안정상태 시각유발전위를 유발시킴을 확인하였으며, 또한 이중 주파수 자극이 안정상태 시각유발전위 정확도를 높이고, 최종적으로 기존 스펠러들에 비해 정보전달률을 향상시켰음을 확인하였다.

결론적으로 제안된 안정상태 시각유발전위 기반 뇌-컴퓨터 인터페이스들은 이중 주파수 안정상태 시각유발전위를 이용하여 시각 피로도를 낮추고 정확도를 향상시켰으며, 주파수 제한 문제를 해소하였다. 이러한 결과들은 안정상태 시각유발전위 기반 뇌-컴퓨터 인터페이스 시스템이 일상 생활에서 더 안정적이고 효과적으로 사용되는데 기여할 것으로 기대한다.

주요어 : 뇌-컴퓨터 인터페이스, 안정상태 시각유발전위, 이중 주파수, 진폭 변조, 하이브리드 뇌-컴퓨터 인터페이스
학 번 : 2009-21075